Publications of the Astronomical Society of the Pacific
105: 693–720, 1993 July

An Atlas of Low-Resolution Near-Infrared Spectra of Normal Stars

ANA V. TORRES-DODGEN AND WM. BRUCE WEAVER

Monterey Institute for Research in Astronomy, 900 Major Sherman Lane, Monterey, California 93940
Electronic mail: 3303p@navpgs.bitnet

Received 1993 March 8; accepted 1993 April 13

ABSTRACT. We present spectra of O to M stars, luminosity classes V, III, and Ib in the wavelength range 5800–8900 Å, at approximately 15 Å resolution. We give identifications of the main spectral features and show that the stars follow well-defined morphological sequences in both temperature and luminosity. This wavelength region and resolution, combined with the high sensitivity of silicon-based detectors, are very useful for spectral classification.

1. INTRODUCTION

The morphological classification of stellar spectra has been one of the most powerful tools in astronomy. The wavelength regions used for classifying stars have naturally followed the available wavelength sensitivity of the most efficient detectors and the capabilities of the spectrographs. Thus, spectral classification of the later half of the 19th century was performed in the visual; however, the advent of photographic emulsions, with their integrating capability, moved the classification region to the blue range of the spectrum. It was in this region that the basis of spectral classification as we know it today was developed at Harvard by W. P. Fleming, A. Maury (first two-dimensional system), and A. Cannon. The modern system was codified by Morgan et al. (1943, MKK) and Morgan and Keenan (1973) between 3900 and 4900 Å, at about 2 Å resolution. Revised spectral types are listed in Johnson and Morgan (1953), Keenan and McNeil (1976), and Morgan et al. (1978). As the ultraviolet (UV) transmission of astronomical optics improved, the MKK system was extended into the terrestrial observable UV (e.g., Abt et al. 1968).

Figure 1 compares the spectral sensitivities and quantum efficiencies of old and current detectors. The region between 5800 and 9000 Å is immediately attractive for an extension of the spectral classification as it lies in the peak of the sensitivity of silicon sensors. There are other advantages in classifying stars in this spectral region. The first is that late-type stars emit most of their light here, so they are more easily and rapidly detected in the near infrared (NIR) than in the blue. Second, highly reddened O to M supergiants and OB stars [$E(B-V) > 1$] are difficult to classify in the MK system because of the long exposure times required, unless large telescopes are used. Third, luminosities are more easily determined in the NIR, and lastly, blue sensitive CCDs are relatively inaccessible to small observatories.

Furthermore, in analogy to the blue spectrum, the NIR region contains many of the lines of the hydrogen Paschen series and its limit, and the Ca II infrared triplet. There are also a number of lines and molecular bands, unique to the region, that are well known for their temperature and luminosity sensitivities. These strong features make this region well suited for objective-prism-quality classification at low resolution of very faint objects. Beyond its attractive spectroscopic features, the NIR is less demanding of the optics of the spectrograph, and less sensitive to interstellar reddening and telluric atmospheric effects such as differential refraction (Filippenko 1982). At 15 Å resolution, strong telluric oxygen and water bands represent confined annoyances rather than major obstructions, especially for early-type stars; they are a more significant problem at higher resolutions and in the spectra of the cooler stars.

Early classification schemes in the NIR include those of Keenan (1957), Keenan and Hynek (1950), who noticed the luminosity dependence of the O I $\lambda\lambda$7774, 8446 lines in the B–G stars, of Sharpless (1956), who derived a NIR classification system for M-type stars at 200 Å/mm, and Nassau (1956) who demonstrated the use of low-dispersion objective-prism spectra in classifying M stars. Parsons (1964) suggested the use of the Paschen lines and the Ca II triplet ($\lambda\lambda$8498, 8542, 8662) as additional criteria for classification of A–F stars. He noted that for these stars, luminosities were more easily determined in the NIR than in the violet. The reverse is true for temperature classification. Bouw (1981) followed Parsons' suggestion to show that for A5 to G0 stars, luminosity classes Ia to II can be classified in the NIR as accurately as in the MK system. These results were not widely applied by astronomers, probably because of the slowness of the required I–N emulsions.

In the last 20 years, less than a score of studies have dealt with spectral classification in the wavelength band 0.6–1.0 μm. Most of them deal with late, cool stars, and many of the earlier ones were photometric systems (e.g., Wing 1970). Andrillat and collaborators (1979 and references therein) are the only ones that describe the spectra of some early-type stars (Of and Be) and show the trends of various spectral lines with MK classes. Gunn and Stryker (1983) published a catalog of stars taken with a multichannel scanner from 3130 to 10800 Å, at 20–40 Å resolution.

Image tube-based systems made NIR spectroscopic-based classification systems feasible. Then, in the 1980s silicon-based detectors started to emerge as the most efficient detectors for this spectral region. Barbieri et al. (1981) used 6 Å resolution Reticon spectra to classify cool stars in the spectral region 7000–9200 Å. Turnshek et al.

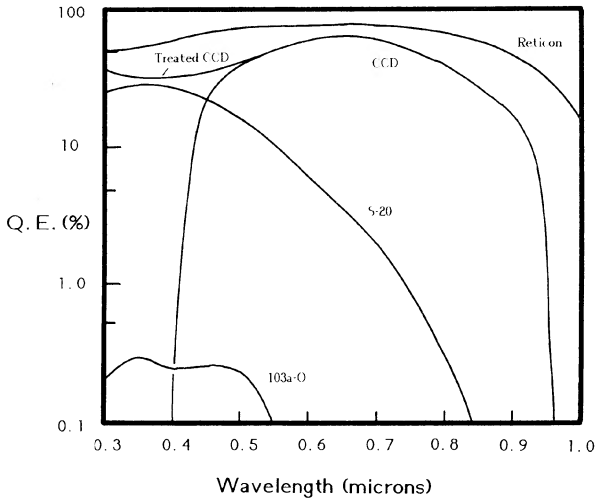

FIG. 1—Quantum efficiency as a function of wavelength for old and new detectors: 103a-O is a blue photographic emulsion, S-20 is a red sensitive photocathode, and the Reticon is unintensified.

(1985) used an intensified Reticon system to extend digital spectra of cool stars (G, K, M, S, and C) to about 8000 Å. Sequences of K and M stars have been observed by a number of investigators, like Schulte-Ladbeck (1988) and Kirkpatrick et al. (1991). Related studies include the work of MacConnell et al. (1992), who are using NIR photometry and spectra in the wavelength range of 6400–8800 Å to survey distant, cool supergiants along the southern Galactic plane.

To date, only Danks and Dennefeld (1993) have completed an atlas of 126 southern O to M MK standards, between 0.58 and 1.0 μm. Their observations were taken with a Reticon at a resolution of 4 Å, about four times better than ours. We have several stars in common with their study, and even at our lower resolution the stars can be classified relatively well in temperature and luminosity, as we will show in Sec. 4.

2. THE NIR CLASSIFICATION PROCESS

The MK process, described in Garrison (1984), consists of deriving a self-consistent and autonomous system of classification. Such systems are autonomous in that they are to be defined completely by the morphology of spectral features in arrays of stellar spectra. The spectra of standard stars are to be arranged in an orderly way, dependent only on their appearance. There is nothing in the process that demands the use of line ratios; these only provide a discriminating technique for distinguishing slowly varying patterns.

The adopted standards define the system. The designers of the system can only indicate those patterns useful in the classification process. Although the classification system can recommend resolutions, wavelength regions, widening (or its digital equivalent, signal-to-noise), etc., these will vary between observatories. As the system is based on the orderly array of standards, this instrumental variability is not significant. *Thus, the present work is primarily a feasibility demonstration.* Researchers using similar instruments can expect a comparable level of success in classifying stellar spectra; in addition, we include a description of spectral features that we found useful in the classification process.

Formally, then, we should apply the MK process by taking NIR spectra, arranging them in sequences, develop a self-consistent set of NIR standards, and assign them a nomenclature. Pragmatically, such a system seemingly unrelated to the MK system would find little use in the astronomical community. Thus, just as the MK system adopted the traditional nomenclature of the preceding efforts in stellar classification, we have adopted the traditional two-dimensional MK classification. In addition, as a preliminary set of standards, we are starting with well-classified stars, primarily the dagger standards from Morgan and Keenan (1973). These are shown in Table 1. We expect these to present a smooth change in characteristics in the NIR with MK class.

Three types of discrepancy with the blue MK system may occur when using the MK standards. Some MK standards may be unusual in the NIR; we intend to use spectra from at least two well-classified stars in each spectral class and note any atypical spectra which we reject. There is also the risk of a more severe problem: that, at the subclass level, the continuously varying sequence in the NIR may not be the same as in the blue. If this does occur, the NIR system must then depart from the blue MK system in order to remain self-consistent. There have been no indications of this in the present data. The third source of discrepancy may arise from the influence of binary companions, especially for stars with unknown spectral type. For example, a red companion might affect the NIR spectrum considerably more than the blue. We will continue to carefully examine these issues for each spectral class in future papers.

3. INSTRUMENTATION AND DATA REDUCTION

All the spectra for this study were taken with the MIRA 36-in. telescope, located on Chews Ridge at an elevation of 5000 feet. The telescope is a classical Cassegrain design with an $f/10$ focal ratio. The spectrograph, mounted at Cassegrain focus, is shown in Fig. 2. It was designed by WBW and built by Frank Melsheimer and WBW in the MIRA shop. The collimator, an off-axis parabola of 380 mm focal length, can be rotated to provide the collimated beam to either of two filter, grating, and camera assemblies. A variety of cameras is available with focal lengths between 55 and 600 mm; the 55 mm focal length commercial camera lens was used for this study. The reduction of collimator to camera is about seven; this makes it possible to use a fairly wide slit and still have good definition in the resulting spectra.[1] The spectrograph entrance aperture is set at approximately 4×8 arcsec which, projected on the 25×425 μm diodes of the 512-element Reticon detector,

[1]This sentence was taken from MKK; it is equally true for our spectrograph today.

TABLE 1
Program Stars

Spectral Type Sequence at Luminosity Class V								Spectral Type Sequence at Luminosity Class III								Spectral Type Sequence at Luminosity Class Ib							
Sp. Type	Ref	Name	HR	HD	V	(B–V)	E_{BV}	Sp. Type	Ref	Name	HR	HD	V	(B–V)	E_{BV}	Sp. Type	Ref	Name	HR	HD/BD	V	(B–V)	E_{BV}
O4 V((f))	1	....	....	46223	7.25	0.22	0.54	.....		....	....	.....	....	...	...	O4 If+	1	....	....	190429A	7.12	0.16	0.48
O6 V((f))	1	....	8023	199579	5.96	0.05	0.37	O6.5 III(f)	1	....	....	190864	7.76	0.18	0.50	O6 I(n)fp	1	λ Cep	8469	210839	5.04	0.25	0.57
O9 V	1	10 Lac	8622	214680	4.88	–0.20	0.11	O9 III	2	ι Ori	1899	37043	2.77	–0.24	0.07	O9.5 Ib	2	19 Cep	8428	209975	5.11	0.08	0.35
B1 V	2,3	ω¹ Sco	5993	144470	3.96	–0.04	0.22	B1 III	3	ο Per	1131	23180	3.83	0.08	0.34	B1 Ib	2	ζ Per	1203	24398	2.85	0.12	0.31
B5 V	3	ρ Aur	1749	34759	5.23	–0.15	0.01	B5 III	3	τ Ori	1735	34503	3.60	–0.11	0.05	B5 Ib	3	67 Oph	6714	164353	3.97	0.02	0.11
B8 V	11	ζ Peg	8634	214923	3.40	–0.09	0.02	B7 III	3	38 Aqr	8452	210424	5.46	–0.12	0.00	B8 Ib	4	13 Cep	8371	208501	5.80	0.73	0.75
AO Va	5	Vega	7001	172167	0.03	0.00	0.00	A0 III	5	α Dra	5291	123299	3.65	–0.05	0	A0 Ib	5	η Leo	3975	87737	3.52	–0.03	0
A4 V	6	β Ari	553	11636	2.64	0.13	0.01	A4 III	6	40 LMi	4189	92769	5.51	0.17	0.05	A3 Iab	4	....	641	13476	6.44	0.60	0.54
A9 V	7	44 Cet	401	8511	6.21	0.23	0	A9 IIIb	7	γ Her	6095	147547	3.75	0.27	0	A9 Ia	7	ε Aur	1605	31964	2.99	0.54	0.40
F2 V	7	78 UMa	4931	113139	4.93	0.36	0.01	F2 III	7	β Cas	21	432	2.27	0.34	0	F2 Ib	7	ν Aql	7387	182835	4.66	0.60	0.42
F5 IV-V	4.	α CMi	2943	61421	0.38	0.42	0.00	F5 II-III	4	....	7495	186155	5.06	0.40	0.00	F5 Ib	4	α Per	1017	20902	1.79	0.48	0.22
F9 V	8	β Vir	4540	102870	3.61	0.55	0	F8 III	4	υ Peg	8905	220657	4.41	0.61	0.09	F8 Ib	4	γ Cyg	7796	194093	2.20	0.68	0.13
G2 Va	9	18 Sco	6060	146233	5.50	0 65	0.02	G2 IIIb	9	84 Her	6608	161239	5.71	0.65	0	G2 Ib	8,9	α Aqr	8414	209750	2.96	0.98	0.10
G5 V	9	κ¹ Cet	996	20630	4.83	0.68	0.00	G5 IIIa	10	ο UMa	3323	71369	3.36	0.84	0	G5 Ib	8,9	9 Peg	8313	206859	4.34	1.17	0.17
G8 V	9	61 UMa	4496	101501	5.33	0.72	0	G8+III	8,9	μ Peg	8684	216131	3.48	0.93	0	G8 Ib	8,9	ε Gem	2473	48329	2.98	1.40	0.26
K0 V	8,9	σ Dra	7462	185144	4.68	0.79	0.00	K0–III	8,9	ι Cep	8694	216228	3.52	1.05	0.04	K0–Ib	9	....	....	33299	6.68	1.58	0.40
K3–V	9	Gl 105	753	16160	5.82	0.98	0.03	K3 III	8,9	δ And	165	3627	3.27	1.28	0.02	K3 Ib	8,9	41 Gem	2615	52005	5.68	1.66	0.24
K7 V	8,9	61 Cyg B	8086	201092	6.03	1.37	0.04	K6 III[a]	9	....	152	3346	5.13	1.60	0.08	.....		....	....	.....	...	...	...
M0.5 V	9	Gl 172	....	232979	8.61	1.41	0	M0–III	9	γ Sge	7635	189319	3.47	1.57	0.00	.....		....	....	.....	...	...	...
M2 V[b]	9	Gl 15A	....	1326A	8.08	1.57	0.10	M2+III	8,9	χ Peg	45	1013	4.80	1.57	0	M2 Iab-Ib	9	KK Per	....	13136	7.76	2.24	0.59
M3–V	9	Gl 752A	....	180617	9.12	1.50	0.03	M3 IIIab	8,9	μ Gem	2286	44478	2.88	1.64	0.04	M3.1 Ib	12	HS Cas	....	+62°207	9.60	...	...

Notes: [a]This is Keenan & McNeil's (1976) K7 III standard.
[b]dM1.5, subluminous in absolute magnitude-color diagrams, strong-line, high-metal abundance star (see text).
Underlined stars are MK standards from Morgan & Keenan (1973) or Morgan, Abt & Tapscott (1978).
When the spectral types have been revised (Ref column), the new type is underlined.
E_{BV}=0 means that the (B–V)o of FitzGerald (1970) yields a negative E(B–V).
References for spectral types: 1. Walborn (1973), 2. Walborn (1971), 3. Lesh (1968), 4. Morgan, Abt & Tapscott (1978), 5. Gray & Garrison (1987), 6. Gray & Garrison (1989b), 7. Gray & Garrison (1989a), 8. Morgan & Keenan (1973), 9. Keenan & McNeil (1989), 10. Keenan & McNeil (1976), 11. Hoffleit & Jaschek (1982), 12. White & Wing (1978).

roughly matches the detector size in the dispersion direction. The projected diode size is 3.8 arcsec. A quartz cylindrical lens, used as the Reticon dewar window, acts as a pseudo-Fabry lens perpendicular to the dispersion by spreading the light over about 200 μm in this direction.

The grating is a 600 line plane grating blazed at 8400 Å.

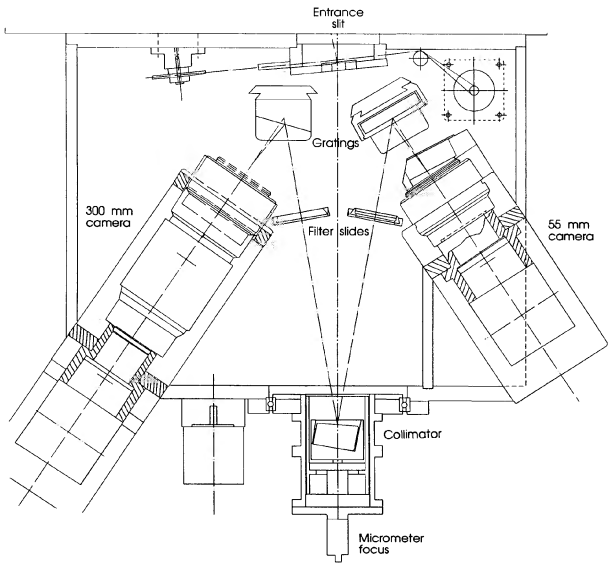

FIG. 2—The MIRA spectrograph.

A GG475 filter is used to suppress the second order. In combination with the 55 mm camera, this provides a dispersion of 6.8 Å per diode. A quartz-halogen lamp provides a flat lamp reference. Wavelength calibration is provided by a Fe–Ar hollow cathode lamp. The full width half maximum measured from the comparison lines is 2.4 diodes, or approximately 15.5 Å. Our final wavelength calibration $\lambda_0 - \lambda$ has a standard deviation of about 1/2 diode, or 3.4 Å, where λ_0 is the laboratory wavelength and λ is the wavelength measured on our spectra.

The detector is a liquid-nitrogen-cooled self-scanned photodiode array: Reticon model RL 512C/17. The high readout noise characteristic of Reticons (less than 1000 electrons for the MIRA system) is not significant in this application because we typically expose to most of diode full well (2×10^7 electrons) where Poisson noise of the

TABLE 2
Spectrophotometric Standards Used from the List of Breger

Star Name	HR	HD	Observer's code
β Ari	593	11636	BAO
ε Ori	1903	37128	HAY
γ Gem	2421	47105	HAY
α Leo	3982	87901	JON
ζ Oph	6175	149757	OKE
ε Aqr	7950	198001	HAY
γ Aqr	8518	212061	OKE
ρ Peg	8717	216735	OKE

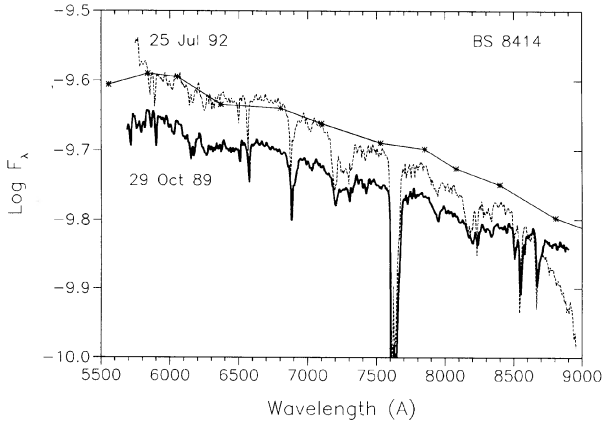

FIG. 3—Two spectra of HR 8414 (G2 Ib) taken at different dates, and the calibration points from Breger (1976), joined by straight lines. The lower spectrum (thicker line) was taken during nonphotometric conditions. The differing continuum at $\lambda > 8500$ Å in the two spectra is typical in our observations.

stellar signal dominates. The large aspect ratio of the diodes makes the device an excellent high signal-to-noise spectrographic detector. The high quantum efficiency of the Reticon, shown in Fig. 1, makes it faster in this regime than a CCD; however, in stars with steep gradients, such as unreddened OB stars, the fainter parts of the spectra do become readout noise limited. There is little in the results presented here that reflect the specific silicon-based sensor used; we expect that the majority of applications will be performed with CCDs.

The primary data reduction was performed with RETINA, an interactive, one-dimensional spectrophotometric data reduction program written by WBW. Wavelength calibrations, dark scans (readout pattern removal by subtracting dark exposures), flat lamp corrections, and spectrophotometric calibration with standard stars were performed for every night's observations. Standard stars were taken from Breger's compilation (1976) and are listed in Table 2 along with the observer whose calibration we used. The calibration of Vega by Tüg et al. (1977) was also used, but instead of using their calibration points in the Paschen area, which are poorly determined, we used the points at 8708 and 9700 Å from Hayes and Latham (1975). At least seven observations of standards were taken every night, and at least three different standard stars. Standard broadband atmospheric corrections, determined observationally for Chews Ridge, are also applied; however, no attempt is made to remove the telluric bands such as the oxygen A and B bands and water bands which fall within our wavelength region, nor the atmospheric emission bands.

Our final calibrated fluxes typically have errors of 10% or more. The errors tend to be largest in the Paschen area, where the calibration points are ill-defined because the spacing of the spectral lines is comparable to the width of the typical filter bandpasses ($\sim$50 Å) used in spectrophotometric systems for flux calibrations, resulting in severe aliasing. Bad seeing, centering errors, and slit orientation (always east–west) (Filippenko 1982; Massey et al. 1992) also contribute to altering the shape of the continuum. An example is shown in Fig. 3, where we have plotted two different observations of HR 8414, one taken on 1989 October 29 and the other one on 1992 July 25, along with Breger's (1976) calibration. The 1989 observation was taken under nonphotometric conditions. Notice the large discrepancy in the continuum shape for the last 300 Å; the fluxes are not well calibrated in the 1992 observation. Unfortunately, such discrepancy is typical in our spectra.

A diode in the neighborhood of 8650 Å often appears "hot" and its value is replaced with the average of its two neighbors.

4. DISCUSSION OF THE SPECTRA

For purposes of demonstrating that the stars follow well-defined morphological sequences in temperature and luminosity in this NIR spectral region, we have chosen to present three stars in each spectral class, spaced as evenly as is possible with the observations that currently exist in our program. For each spectral type we also present spectra of a main sequence, a giant, and a supergiant star, again whenever possible.

Throughout this section we will use the following terminology: spectral class, or class, for O, B, A, etc.; spectral type for A1, F2, G5, etc.; MK type whenever the spectral type and luminosity class are specified. At this point we stress that we are only illustrating the NIR, low-resolution characteristics of the MK standards.

Table 1 lists the stars whose spectra are shown here, along with their V magnitude, $(B-V)$ color, and color excess. The intrinsic colors for each MK type were taken from FitzGerald (1970). When an entry of 0 is given for $E(B-V)$, it means that $(B-V)_0 > (B-V)$, resulting in negative $E(B-V)$.

We present the NIR spectra in the following way: Figs. 4–7 show the plots of the main-sequence stars listed in Table 1, luminosity class III stars are plotted in Figs. 8–11, and stars of luminosity class Ib or higher are shown in Figs. 11–14. Figures 16–22 show the luminosity dependence of one spectral type in each spectral class. Luminosity sequences for other spectral types can be compared by looking at the three spectra (V, III, and Ib) in the corresponding Figs. 4–15.

The spectra are presented as the $\log(F_\lambda)$ plus an arbitrary constant, permitting the line strengths to be easily compared by eye in all plots. The color excesses are given in parentheses below the spectral type or luminosity class, so that the slope of the continuum and the strength of the Na I λ5893 line are not confused with the contribution of the interstellar medium.

The extent of the strongest telluric bands is marked at the top portion of the plots, with the Earth symbol. These are due to water vapor ($\lambda\lambda$7186, 7273 and $\lambda\lambda$8164, 8177, 8227, 8282), and molecular oxygen (α band at 6277 Å, B band at 6867, 6900 Å, and A band at 7600, 7632 Å). Telluric features are weakly present at almost all wavelengths in our spectral range. We have no problems detecting the water bands between 7800 and 8100 Å, whose

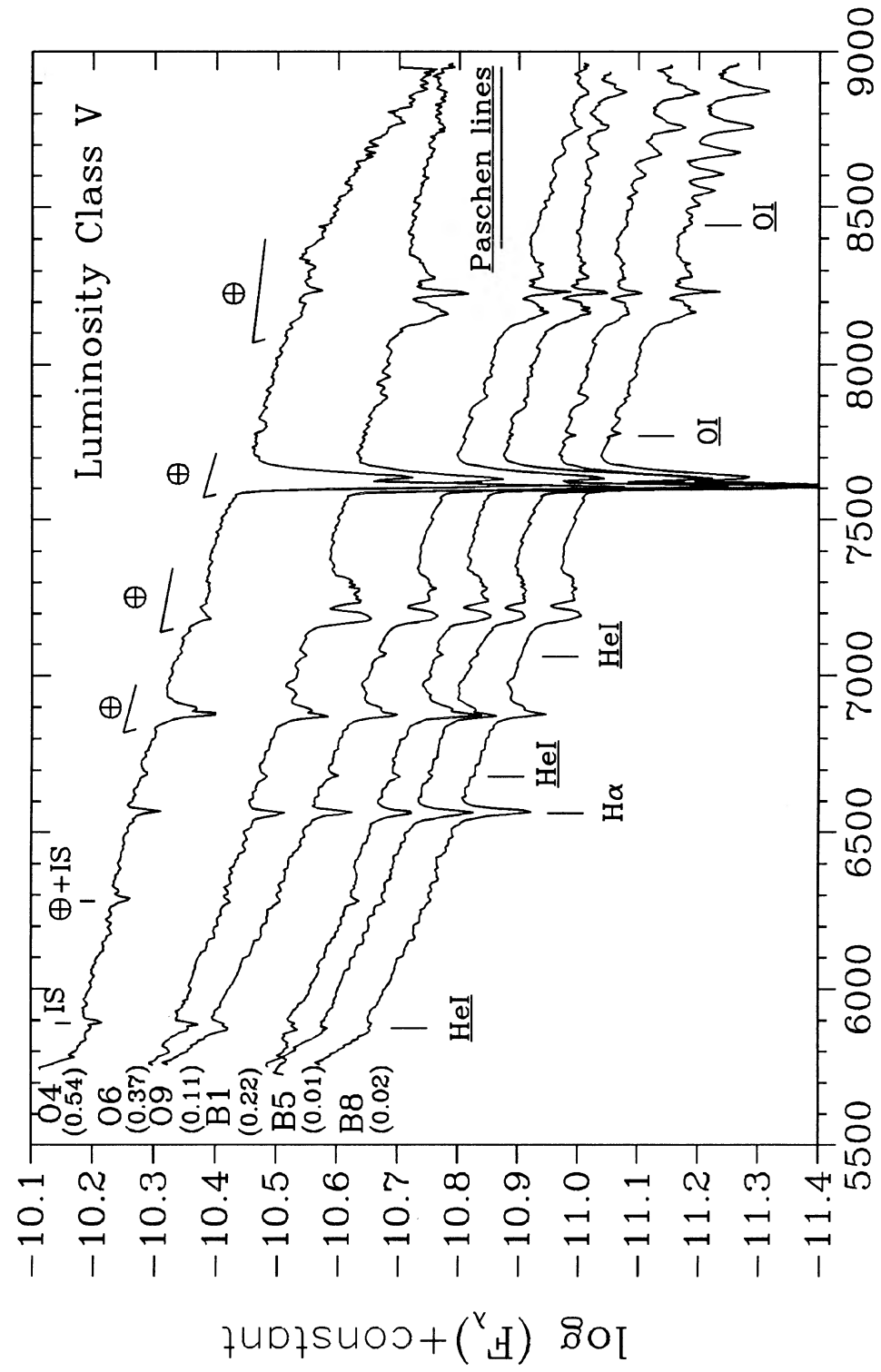

FIG. 4—Temperature sequences for O and B stars at luminosity class V. Each spectrum has been shifted vertically by an arbitrary constant. The main lines have been identified in the bottom portion of the figures. Underlined identifications mean that the feature changes with temperature. Interstellar lines are marked at the top of the figure as IS, and telluric bands are shown as the Earth symbol. The color excesses are given in parentheses under the spectral type, so that the slope of the continuum, and the strength of the Na I λ5893 are not confused with the interstellar contribution.

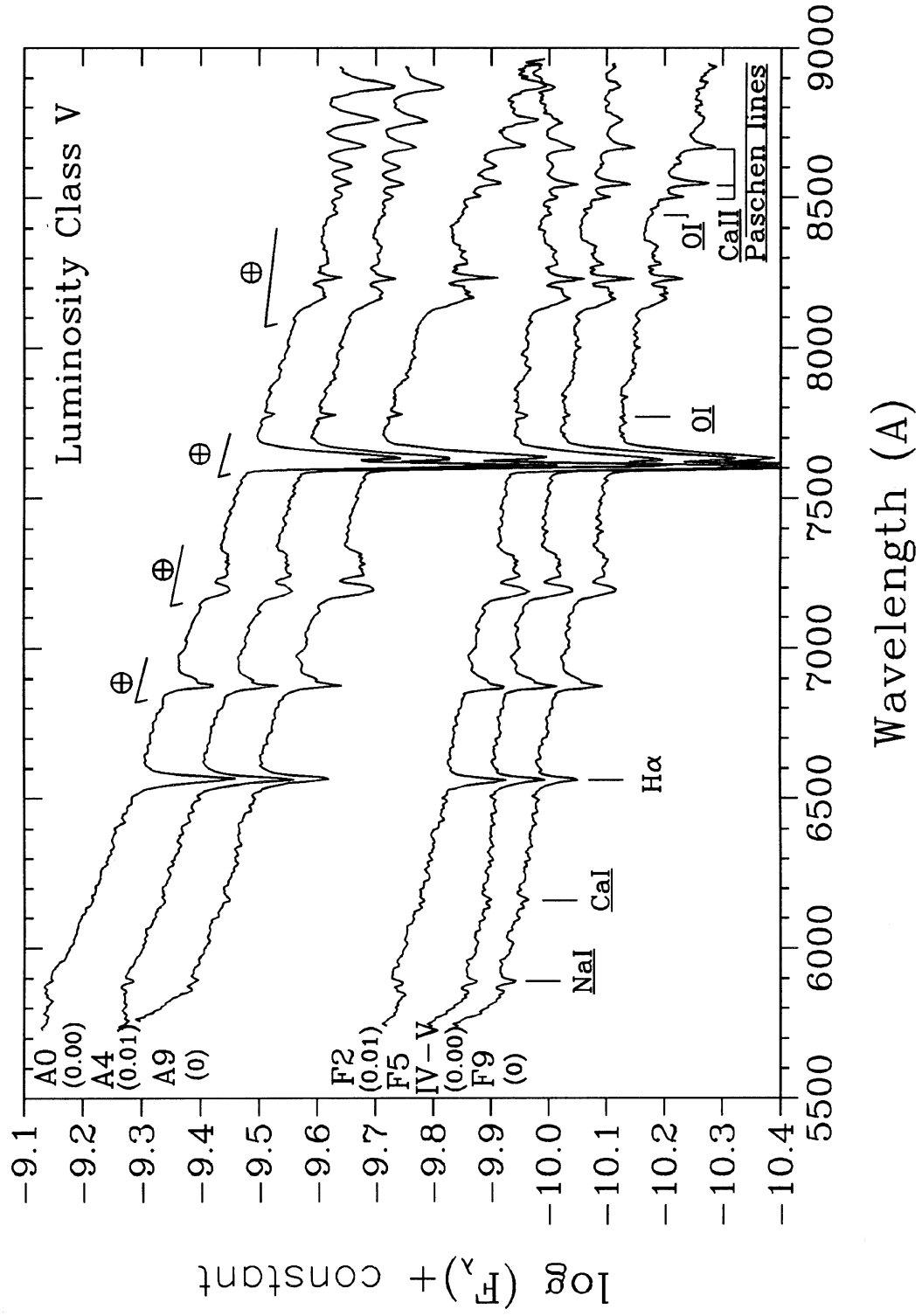

FIG. 5—Same as Fig. 4 but for A and F stars.

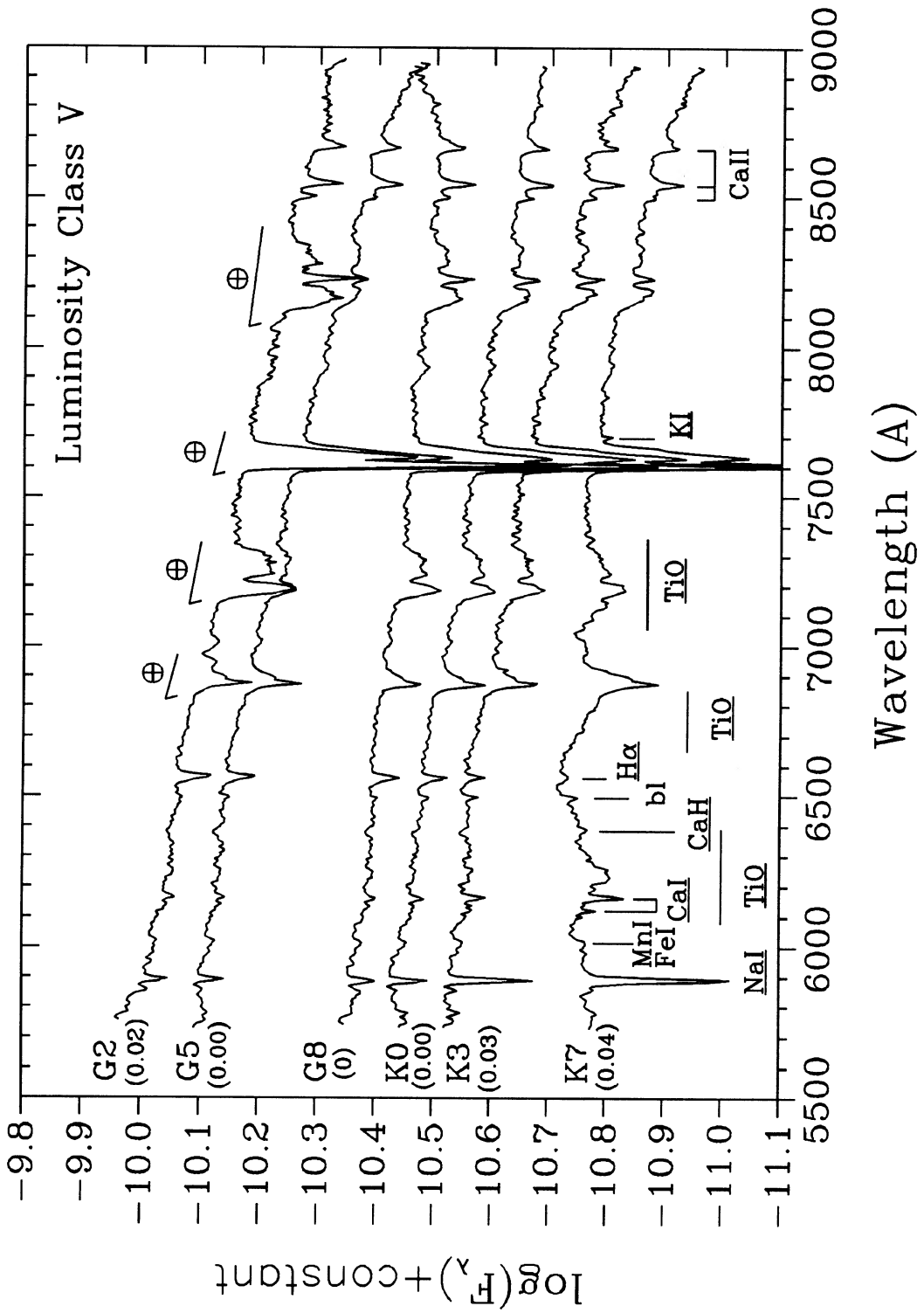

FIG. 6—Same as Fig. 4 but for G and K stars.

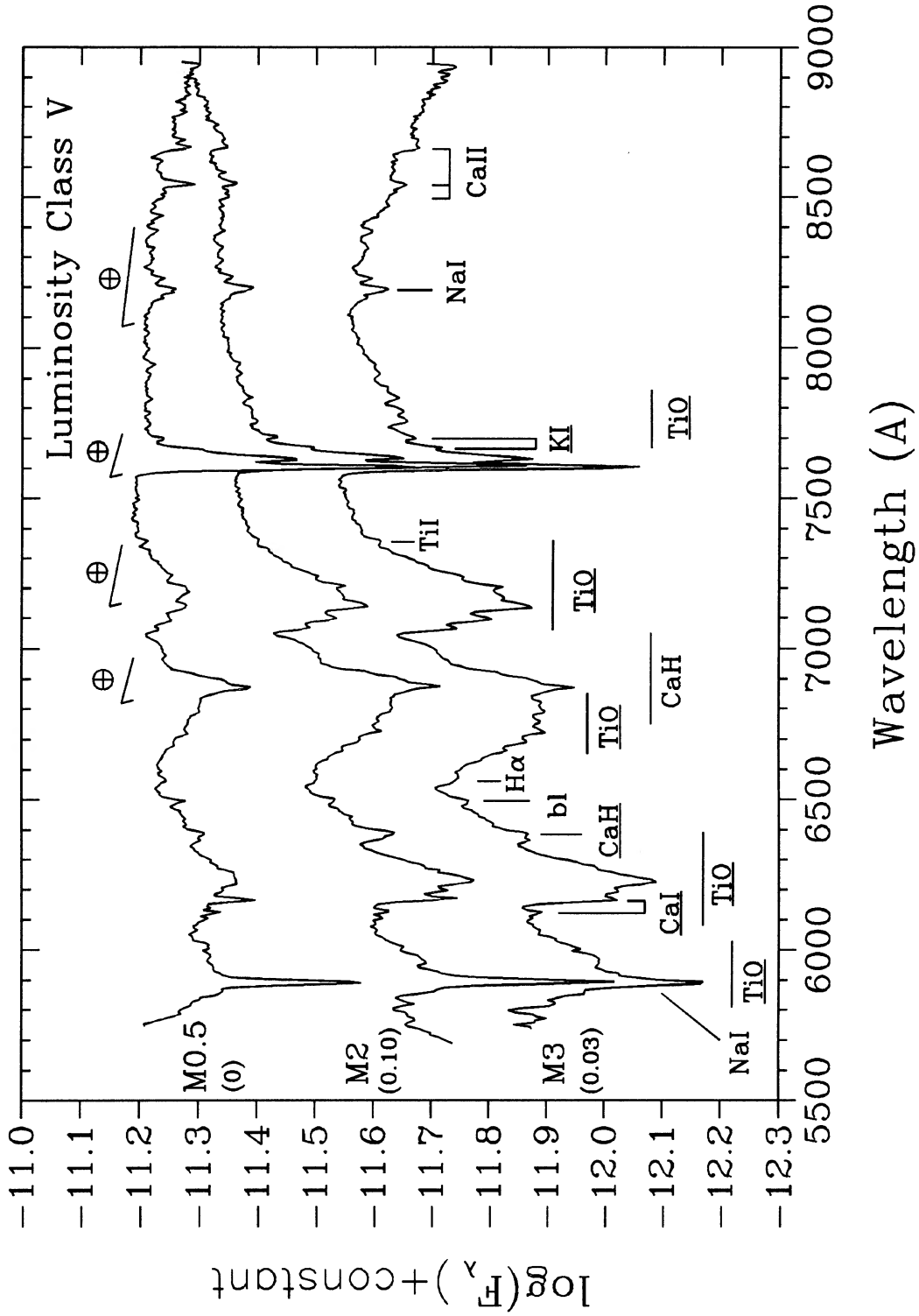

FIG. 7—Same as Fig. 4 but for M-type stars. The M2 V star, classified by Keenan and McNeil (1989) is subluminous in absolute magnitude-color diagrams (see text). The strong CaH band indicates that this is indeed the case.

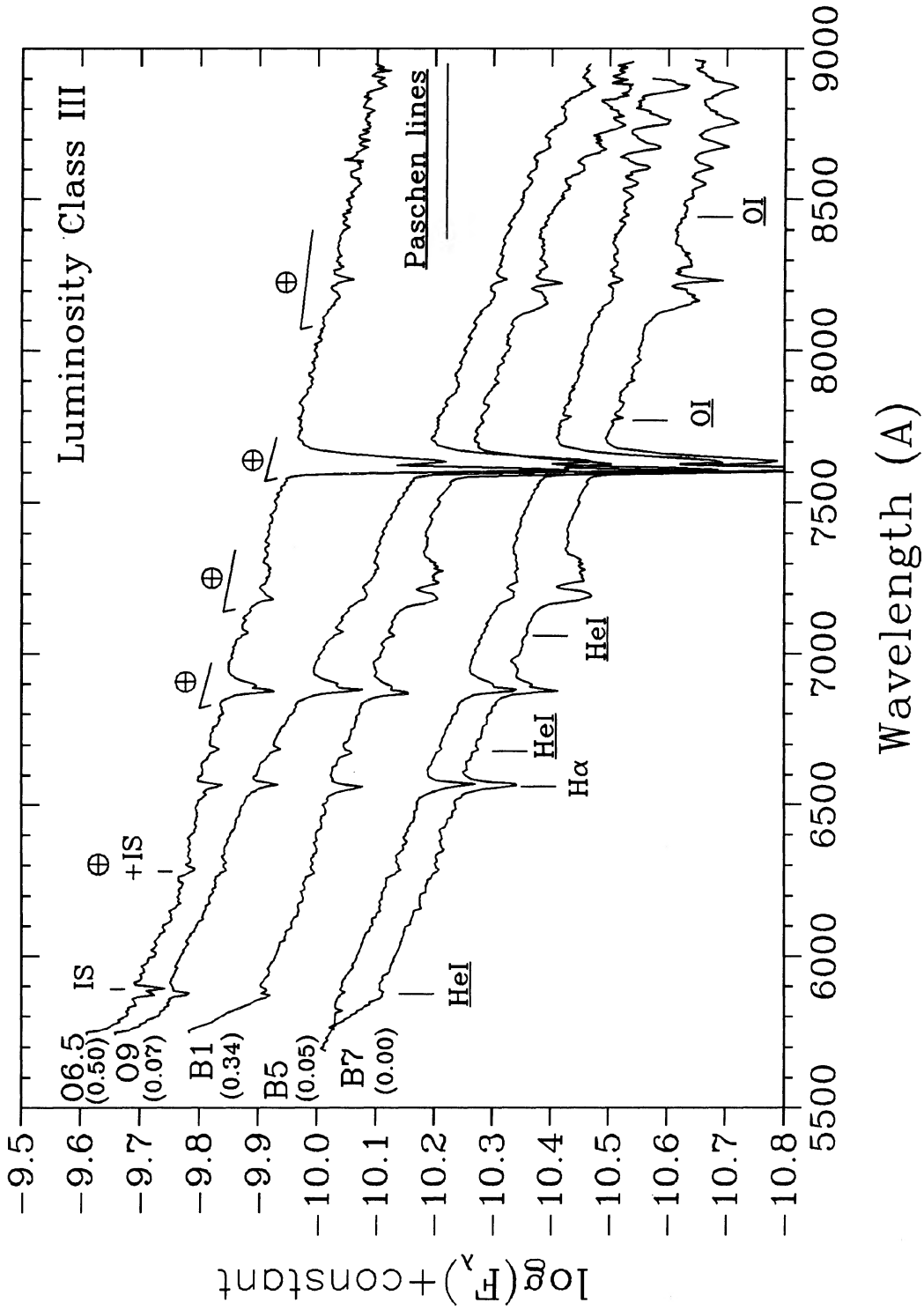

FIG. 8—Temperature sequences for O and B stars at luminosity class III. Each spectrum has been shifted by an arbitrary constant. The legend and symbols are the same as in Fig. 4.

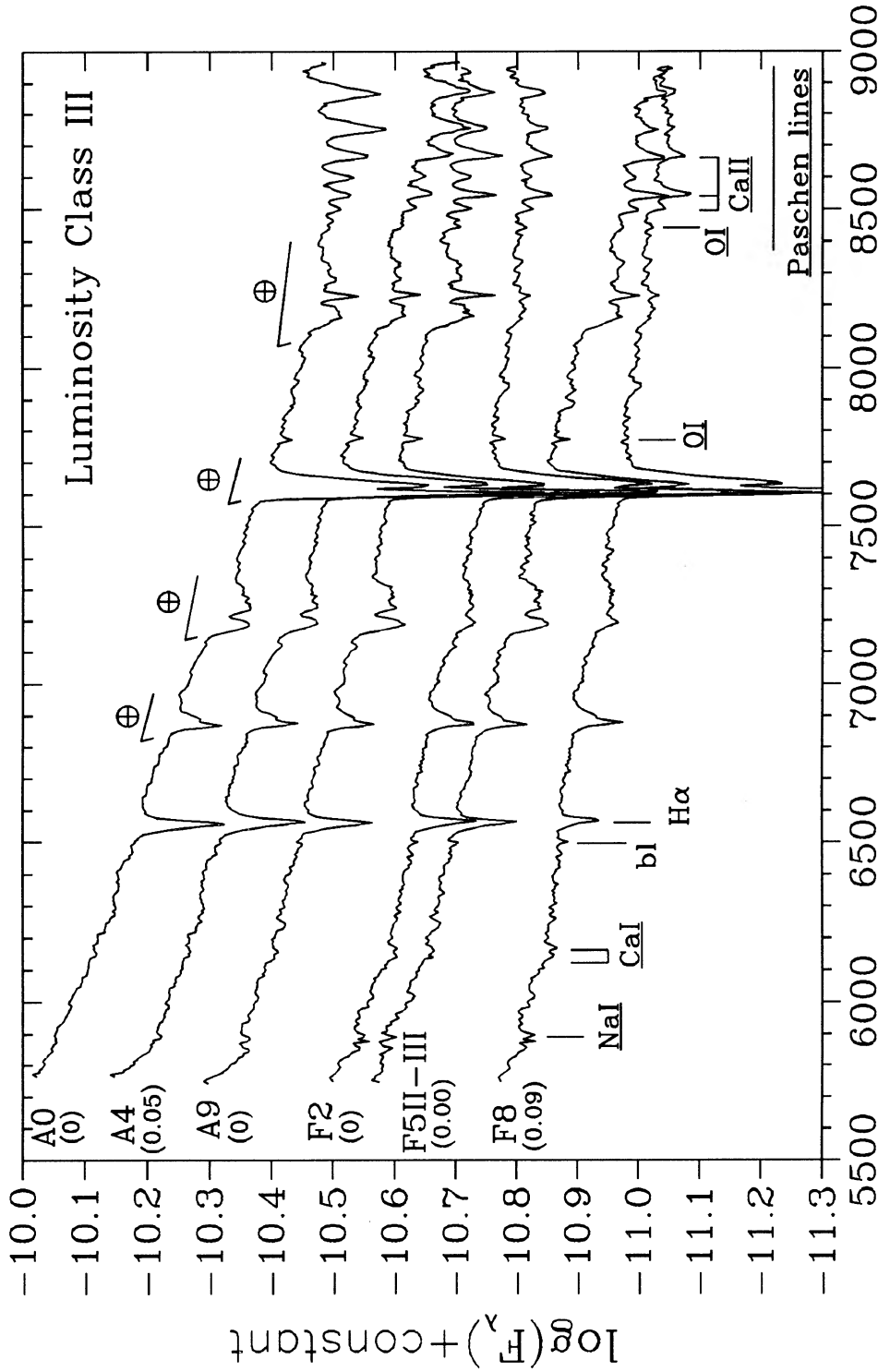

FIG. 9—Same as Fig. 8 but for A and F stars.

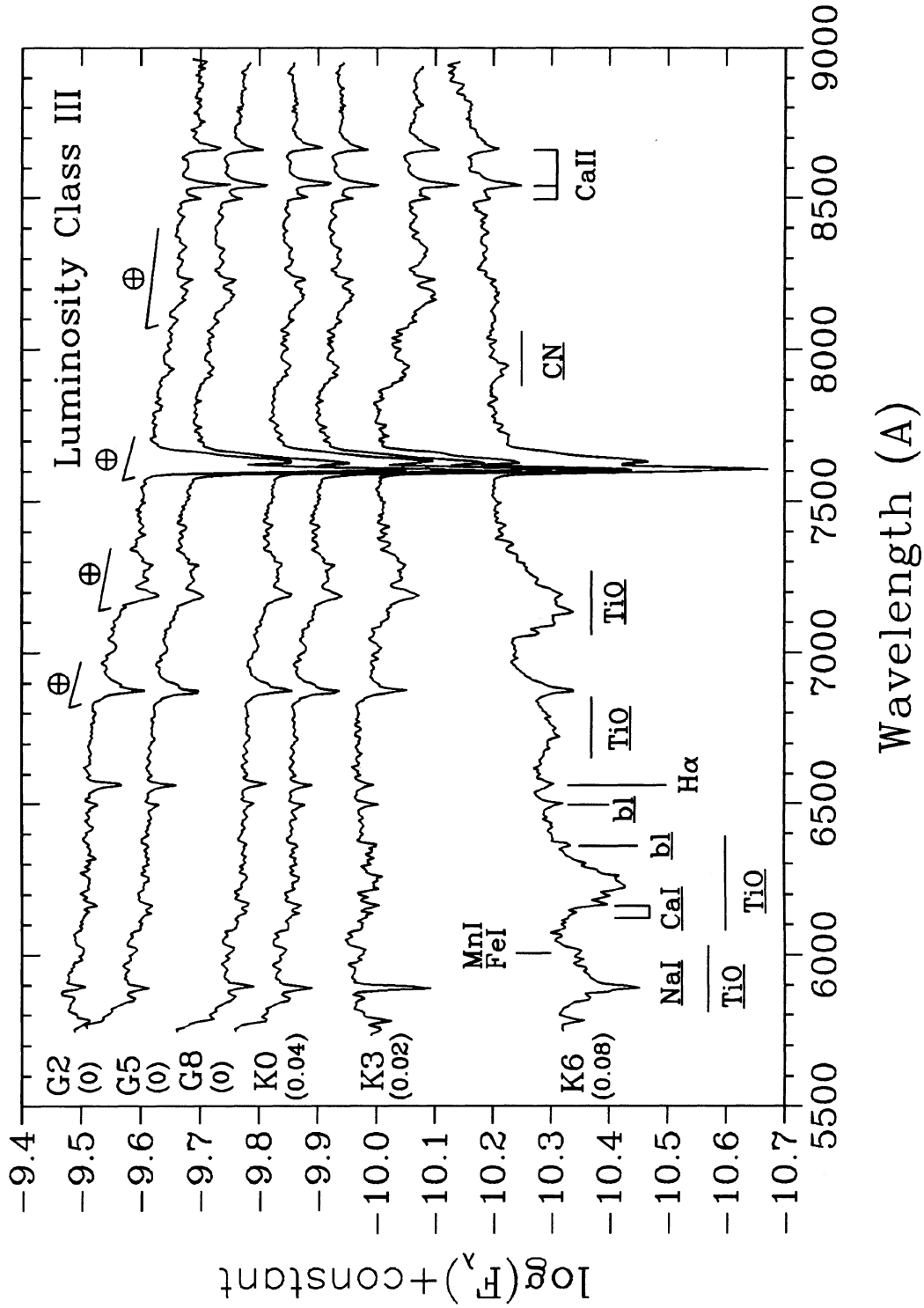

FIG. 10—Same as Fig. 8 but for G and K stars.

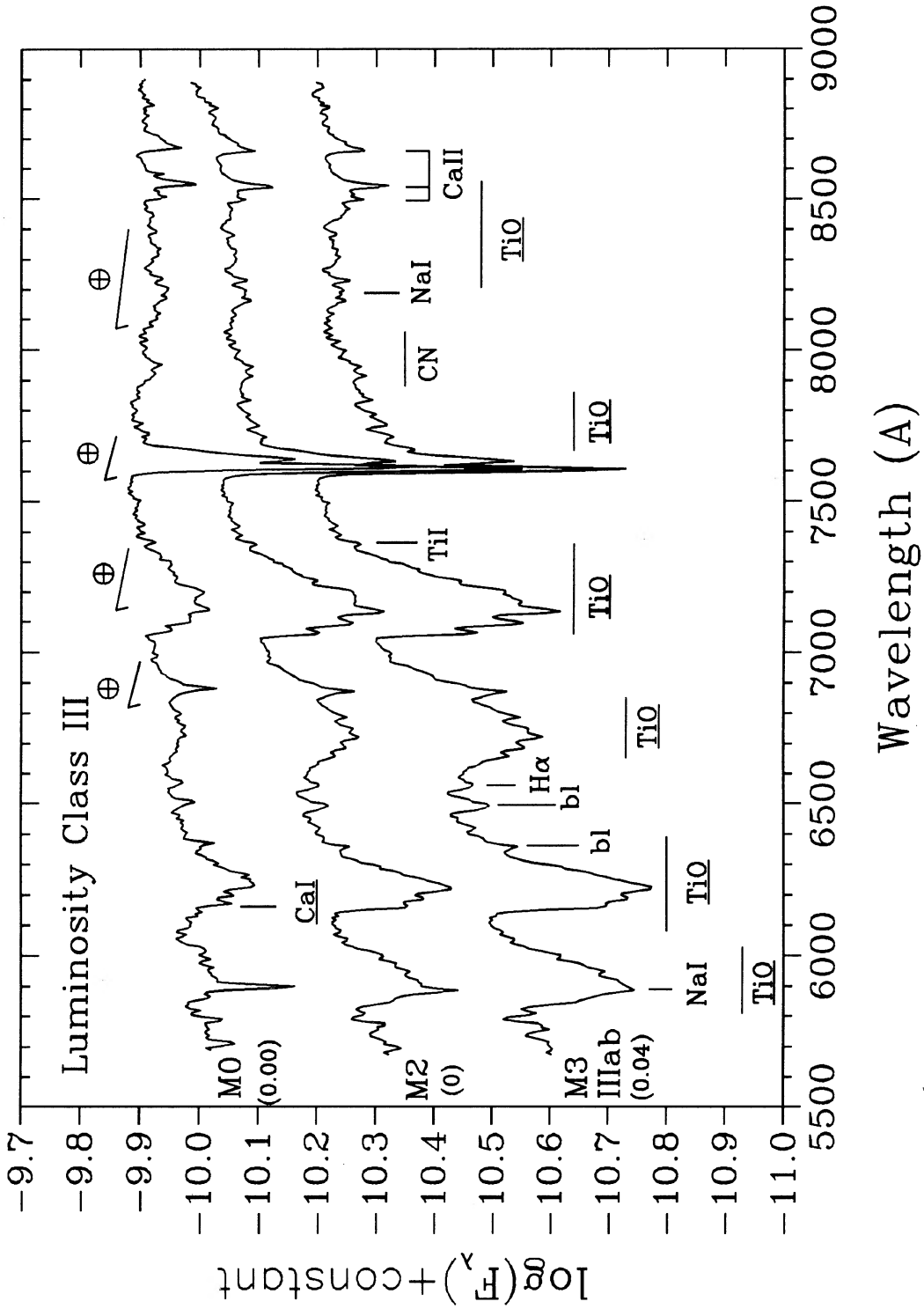

FIG. 11—Same as Fig. 8 but for M-type stars.

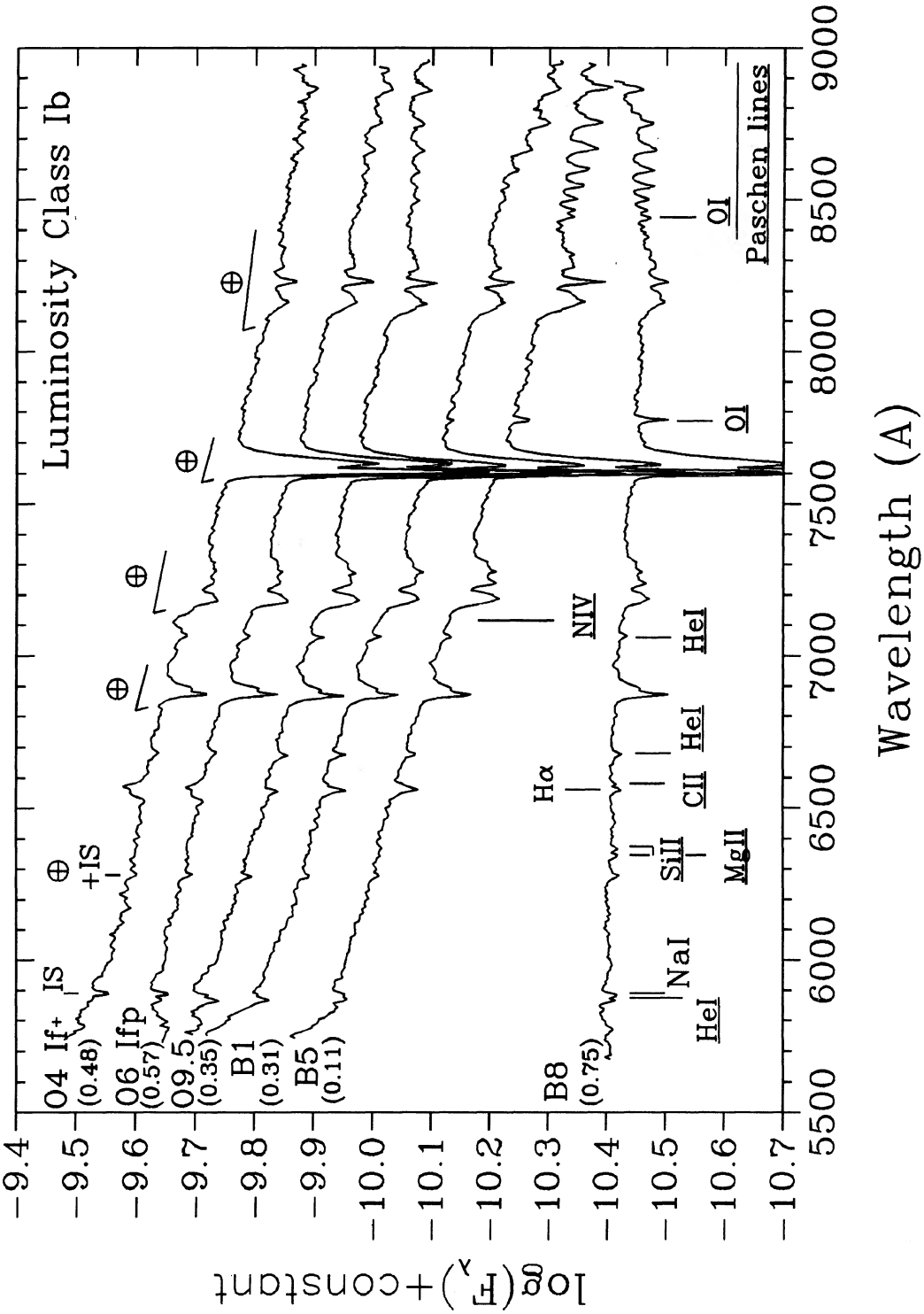

FIG. 12—Temperature sequences for O and B stars at luminosity class Ib or higher. Each spectrum has been shifted by an arbitrary constant. The legend and symbols are the same as in Fig. 4.

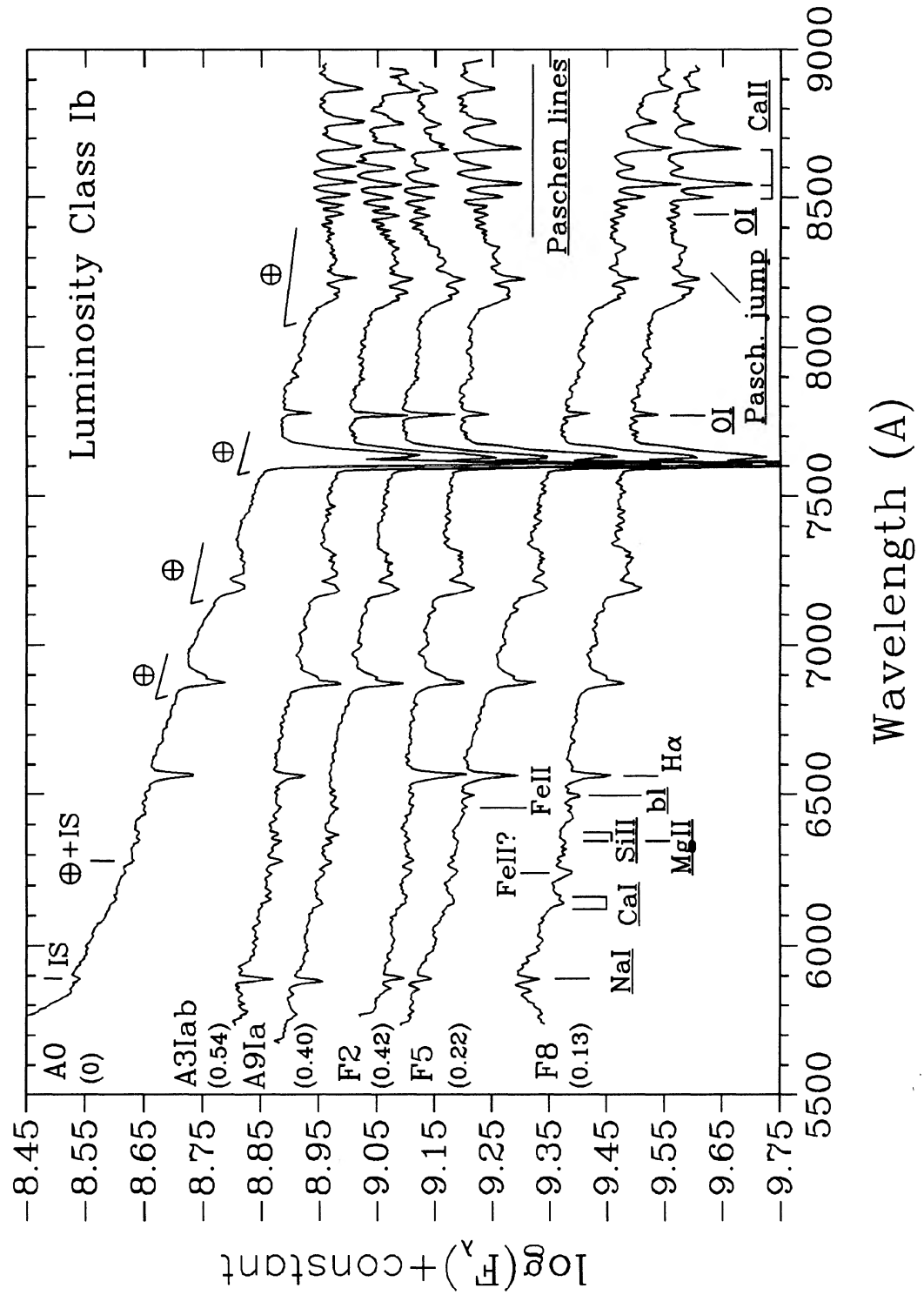

FIG. 13—Same as Fig. 12 but for A and F stars.

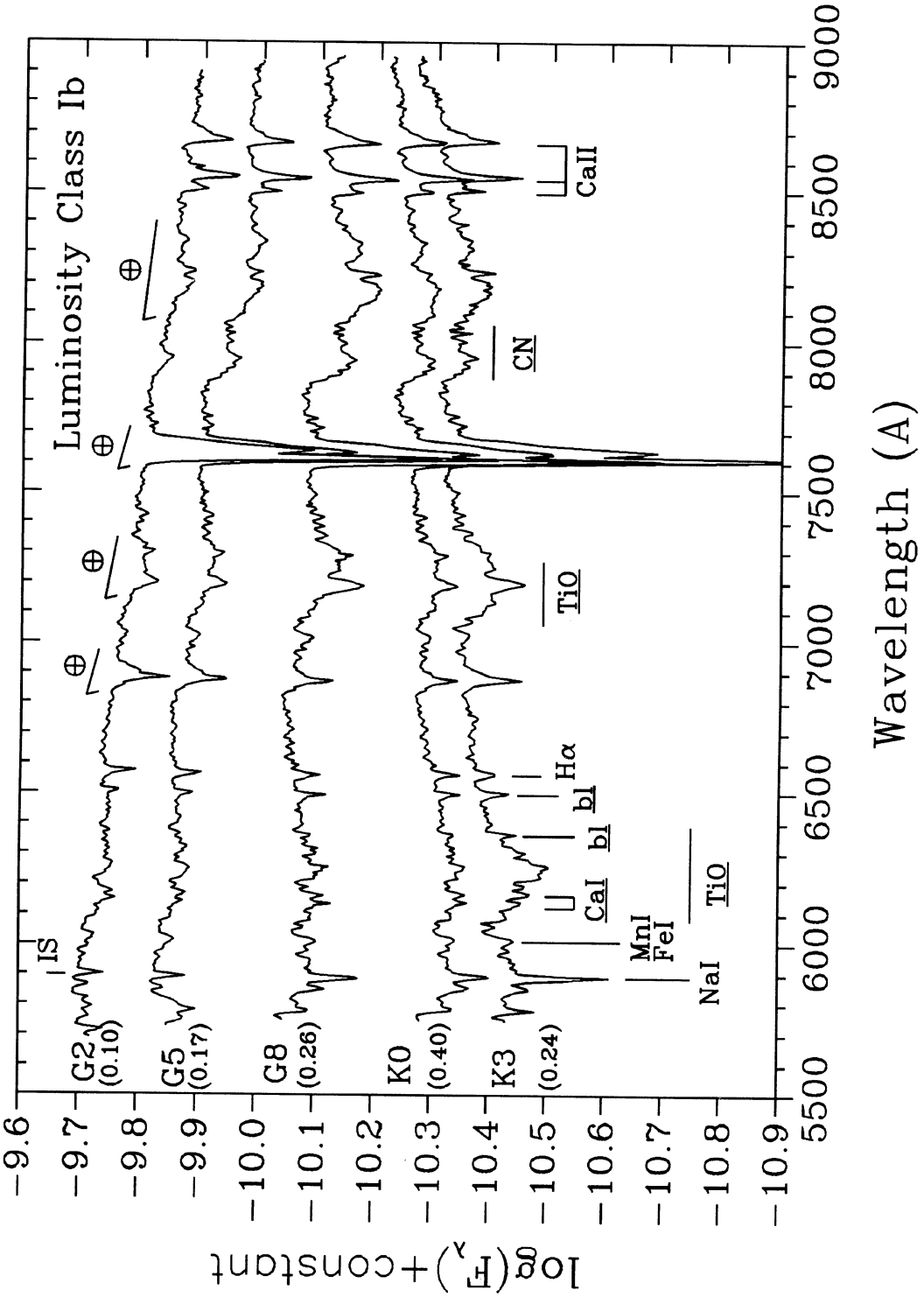

FIG. 14—Same as Fig. 12 but for G and K stars.

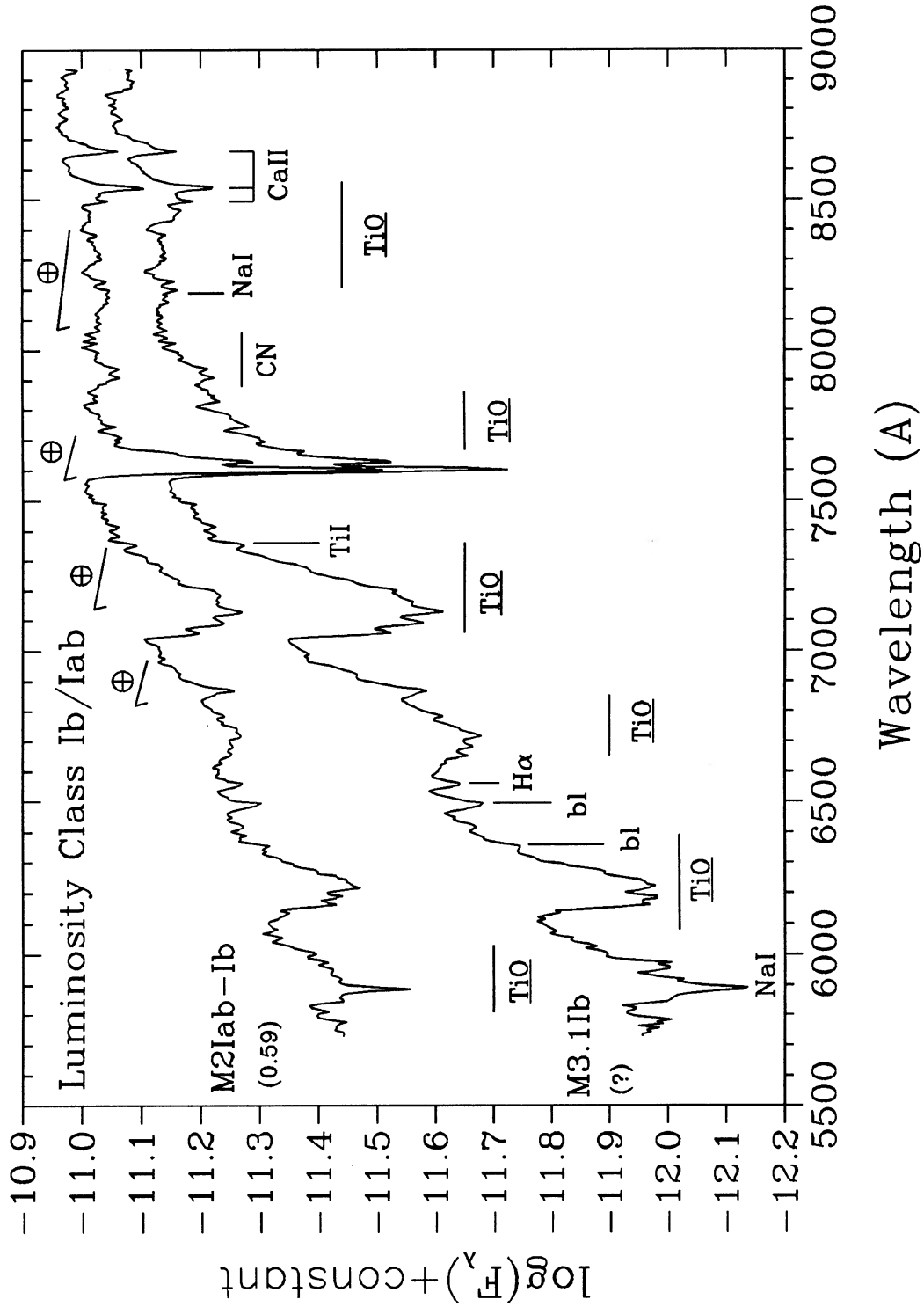

FIG. 15—Same as Fig. 12 but for M-type stars.

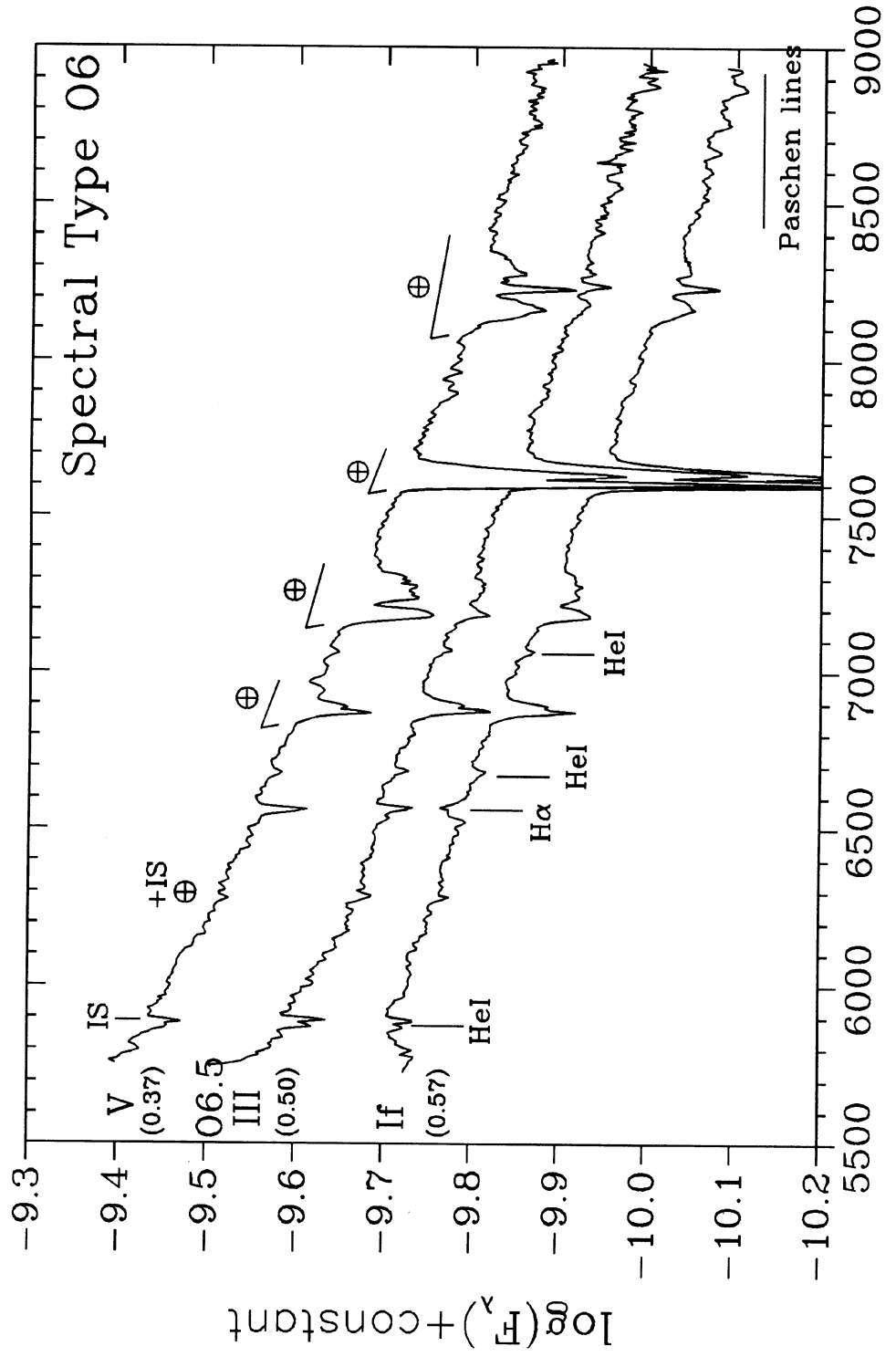

FIG. 16—Luminosity sequence at spectral type O6. Same symbols as in Fig. 4, except that underlined identifications means that the feature changes with luminosity.

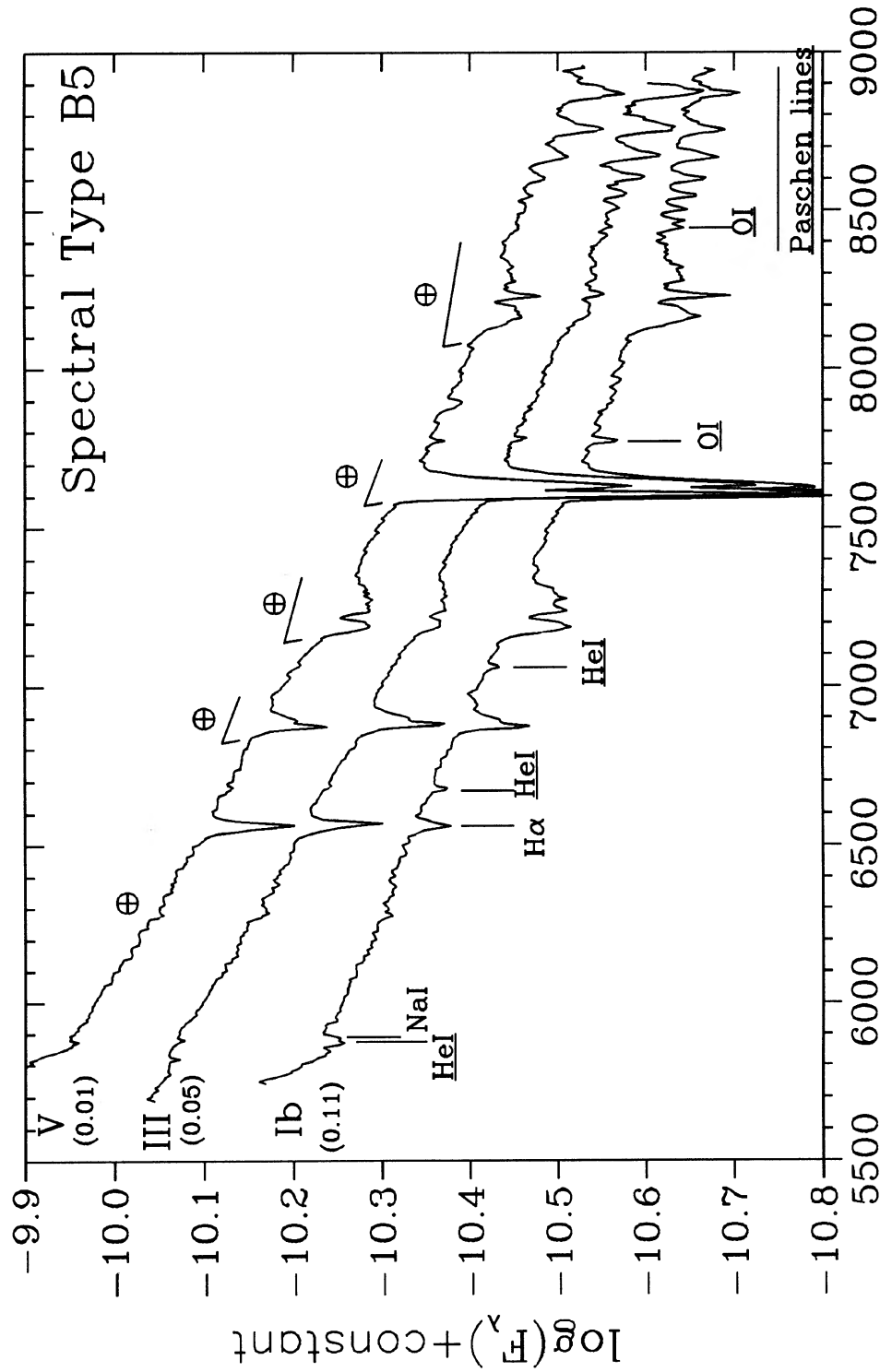

FIG. 17—Luminosity sequence at spectral type B5. The symbols are the same as in Fig. 16.

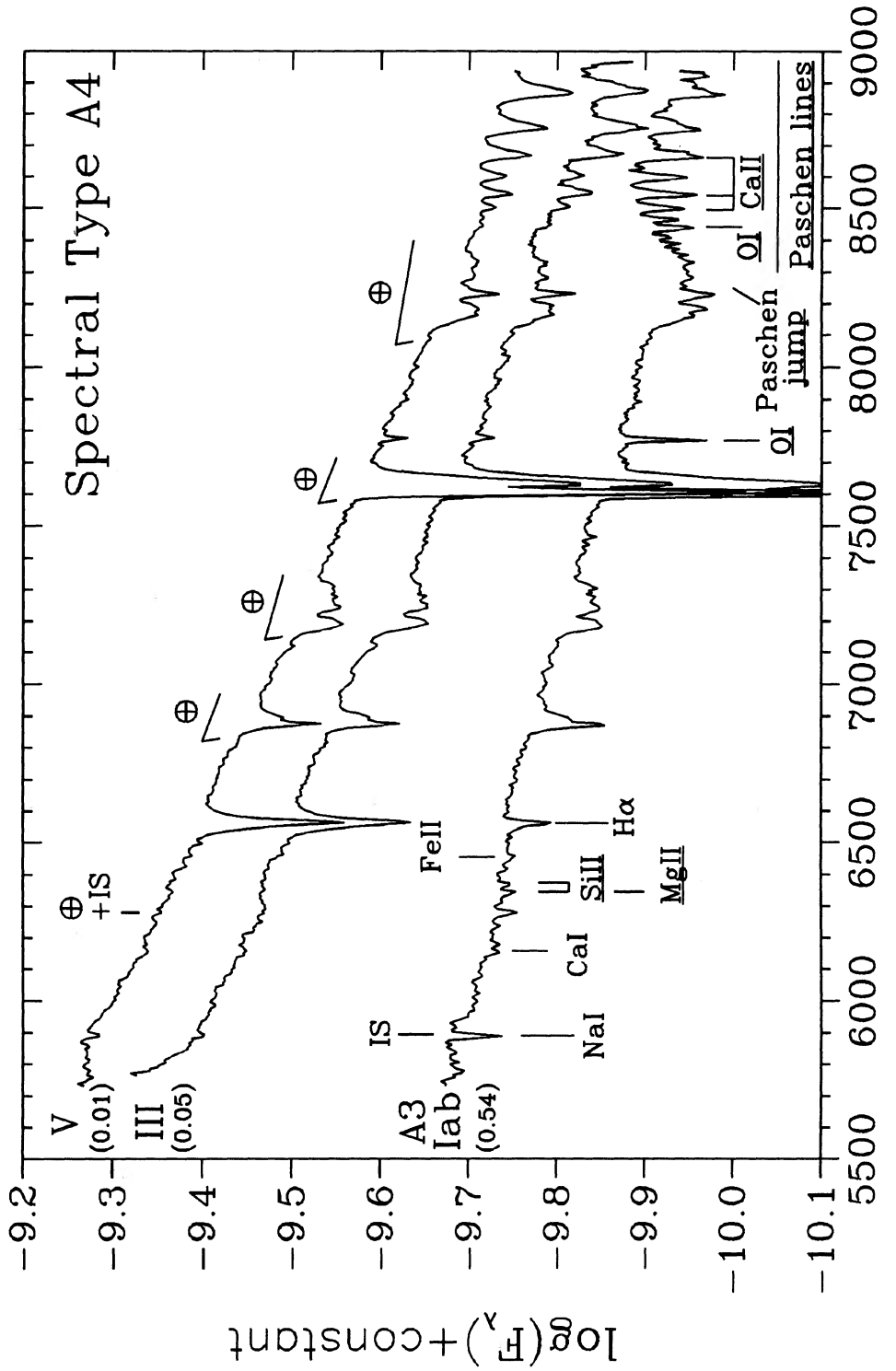

FIG. 18—Luminosity sequence at spectral type A4. Same symbols as in Fig. 16. Interstellar Na I contaminates the stellar Na I line of the supergiant star.

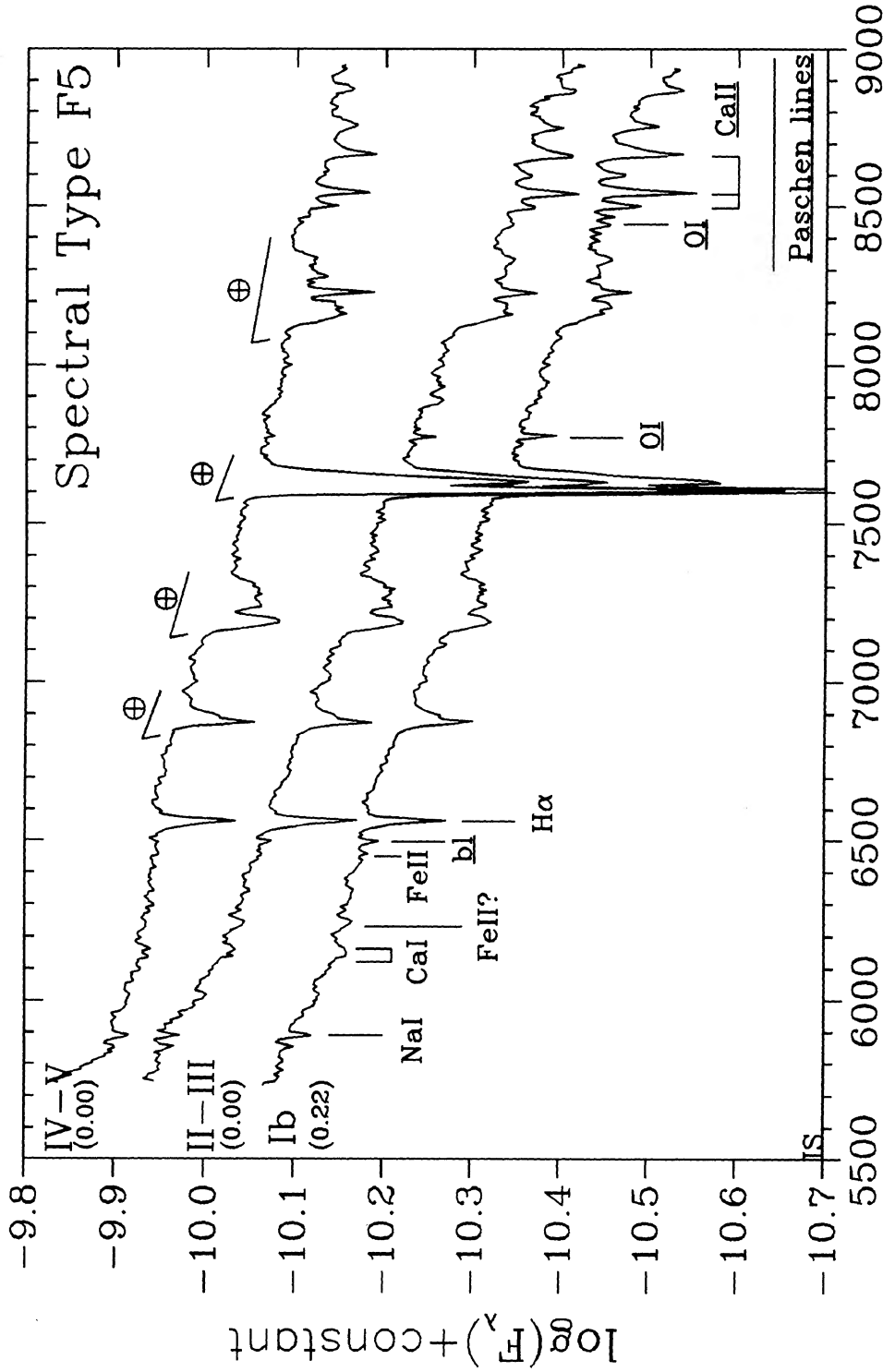

FIG. 19—Luminosity sequence at spectral type F5. The symbols are the same as in Fig. 16.

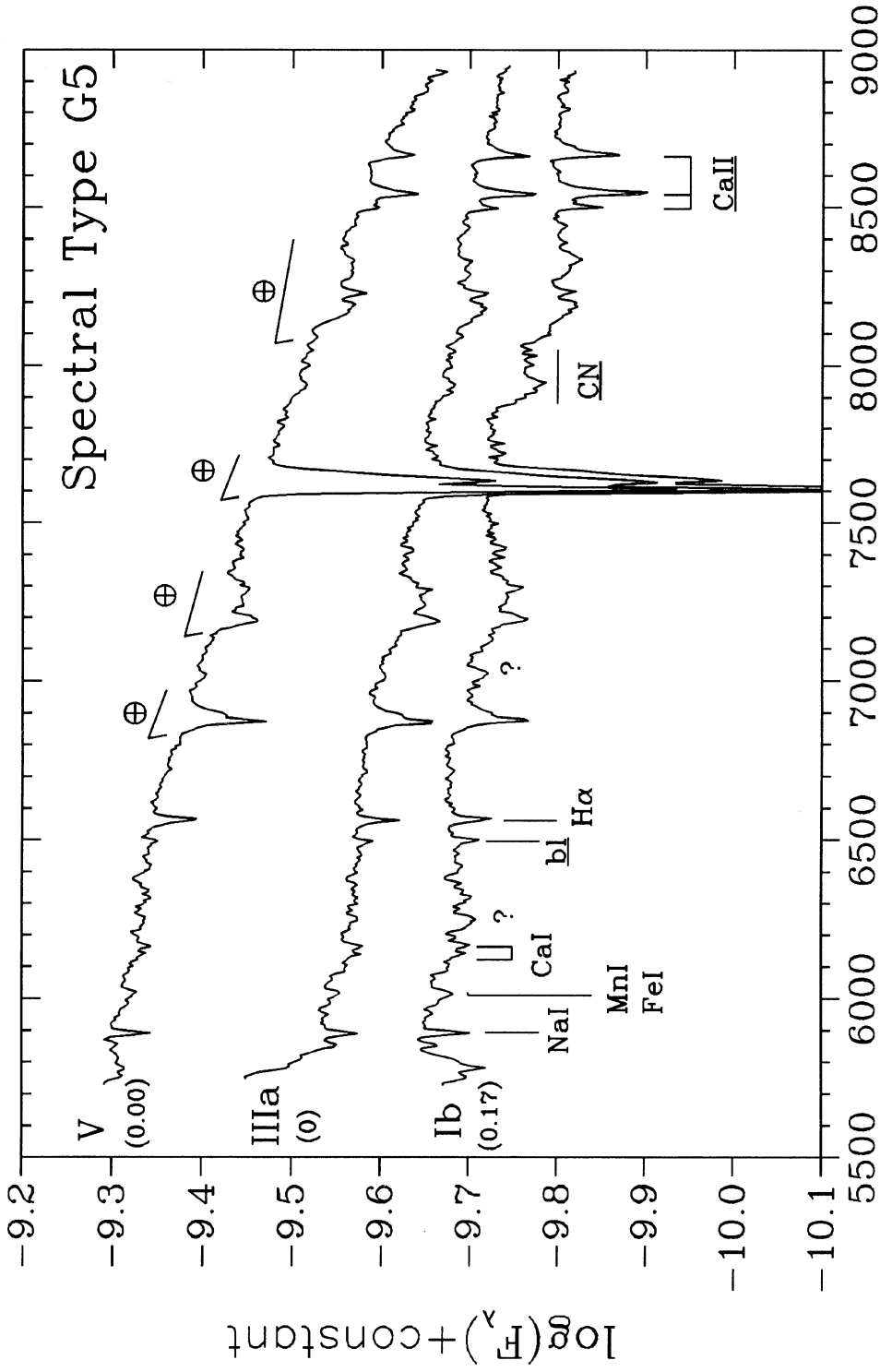

FIG. 20—Luminosity sequence at spectral type G5. The symbols are the same as in Fig. 16. A small contribution of interstellar Na I λ5893 is present in the supergiant star.

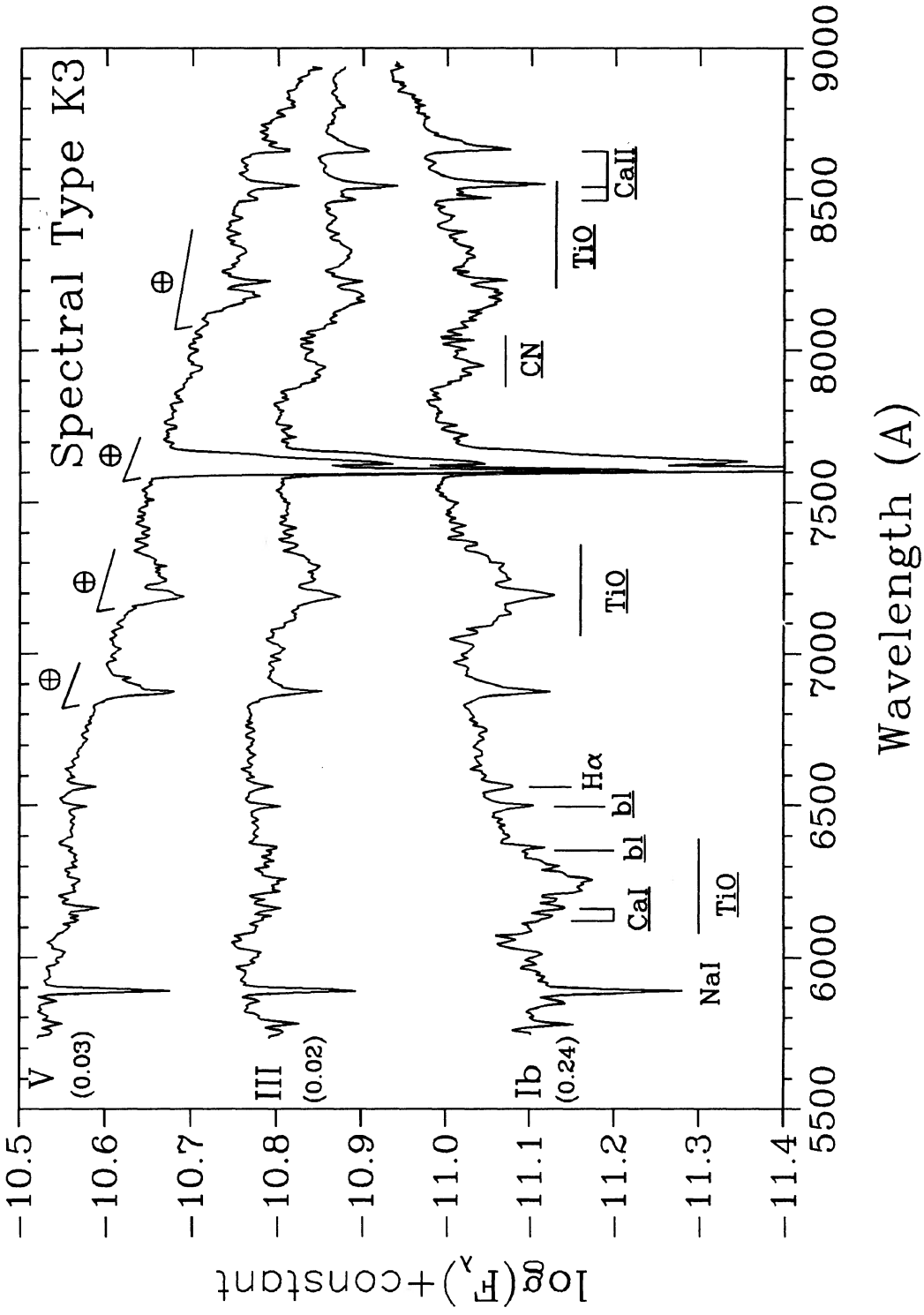

FIG. 21—Luminosity sequence at spectral type K3. The symbols are the same as in Fig. 16. The Na I λ5893 line of the main-sequence star is much deeper than that of the giant.

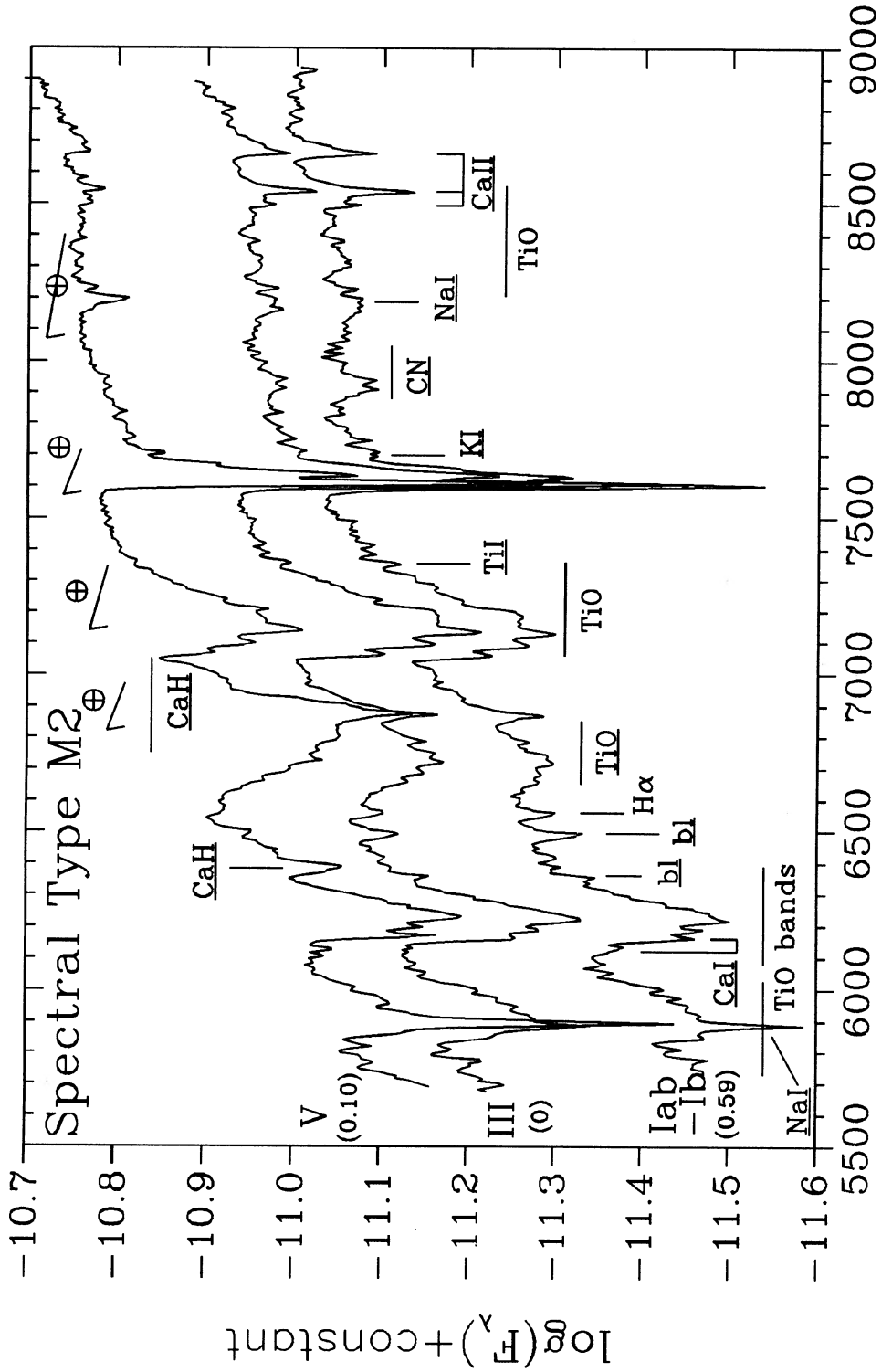

FIG. 22—Luminosity sequence at spectral type M2. The symbols are the same as in Fig. 16. A small contribution of interstellar Na I λ5893 is present in the supergiant star.

strengths do not seem to correlate with the strength of the strong water bands mentioned above. Interstellar lines are marked on the top of the plots as IS, they are the Na I $\lambda\lambda$5890, 5896 doublet (not resolved here) and the λ6284 band. Stellar features are marked at the bottom of the plots. They are underlined if they show a temperature dependence in Figs. 4–15, or a luminosity dependence in Figs. 16–22.

Table 3 lists the stellar lines and features identified in the figures and explains their trends, both with spectral type and luminosity class. The horizontal arrows indicate the direction in which a line strengthens in the luminosity dimension, while the vertical arrows point in the direction in which a line strengthens in the temperature dimension. We do not consider the effects of chemical composition yet, which we expect to be moderate at this resolution.

Notice that many lines are underlined in the spectral type (temperature) plots as well as the luminosity plots.

TABLE 3
Luminosity and Temperature Dependence of the Main Spectral Lines Present in the Red/NIR*

	Feature	Luminosity Class V	Luminosity Class III	Luminosity Class Ib
O	He I $\lambda\lambda$5876,6678,7065	Present in all O-stars. Appear weakest in the O4V star and strongest in the O9 Ib		
	Hα λ 6563	May be variable, therefore not used as a classification criterion ← ↓		Frequently in emission
	N IV λ7117	Not present		Present only in the O4 If+ star, in emission
	Hydrogen Paschen lines	Not enough signal detected in the early O-stars, clearly present in the O9 and O6 If stars		
B	Na I λ5893	Blend of stellar and interstellar lines		
	He I $\lambda\lambda$5876,6678,7065	λ5876 is the strongest of the three lines, λ 7065 not present in the latest B-stars ↑		↑ Present in all B-stars, stronger than in V or III stars
	Si II $\lambda\lambda$6347,6371	Not present		Present only in the B8 star
	Mg II λ6347	Not present		Present only in the B8 star
	Hα λ 6563	May be variable, should be used with caution ← ↓		
	C II λ6580	Not present		Weak, present only in the B8 star
	O I $\lambda\lambda$ 7774,8446	→ ↓		
	Hydrogen Paschen lines	broader ← — — — —		narrower, can resolve more lines in the series ↓
A	Na I λ5893	↓ Weak		Contaminated by interstellar contribution
	Ca I λ6162	Present only in the A9 stars		Present by A3 Iab
	Si II $\lambda\lambda$6347,6371	Not present		↓ λ6347 blended with Mg II
	Mg II λ 6347	Not present		↓ ? Blended with Si II
	Fe II λ 6456	Weak, present in all but A0 V and A0 III		
	Hα λ6563	↑		Can be variable, use with caution
	O I $\lambda\lambda$7774,8446	→		
	Ca II $\lambda\lambda$8498,8542,8662	Not present in the A0 stars → broader ← — — — — — — narrower ↓ (strengthen relative to the Paschen lines)		
	Hydrogen Paschen lines	broader ← — — — — — narrower, can resolve more lines in the series ↑		
	Paschen jump	Not present		Present in all, weakest at A0

*The lines strengthen in the direction of the arrow: → (←) strengthen (weaken) with luminosity; ↓ (↑) strengthen (weaken) with later spectral type

TABLE 3
(Continued)

	Feature	Luminosity Class V	Luminosity Class III	Luminosity Class Ib
F	Na I λ5893	↓		↓ Contaminated by interstellar line
	Ca I λλ6122,6162	Present in all		
	Fe II blends (and more?) λ~6242 Å, broad feature	Present but weak	Present	↓
			→ ?	
	Fe II λ6456	Weak, present in all		
	Fe I, Ca I (and more?) λ6497	→	→	→
	Hα λ6563	↑	↑	↑
	O I λλ7774,8446	→	→	→
		↑ Very weak or absent at F8-F9		
	Ca II λλ8498,8542,8662		→	→
			↓ (strengthen relative to Paschen lines)	
	Hydrogen Paschen lines	broader ← — — — — —		narrower, can resolve more lines in the series
		↑		
G	Na I λ5893	Present in all	↓ ?	
	Mn I, Fe I λ~6015 Å	→	→	→
	Ca I λλ6122,6162	→	→	→
	Ba II, Fe I, Ca I λ6497	→	→	↓
	Hα λ6563	↑ (slightly)		
	CN λ7878-8068	Present?	→	→
	Ca II λλ8498,8542,8662	→	→	→
K†	Na I λ5893	↓		
	TiO λ~5847-6058	Not present	Present only in the K6 star	Very weak or absent in K0, weak in K3
	TiO λ~6080-6390	Present only in the K7 and K6 stars		Very weak or absent at K0, present at K3
		→		
	Ca I λλ6122,6162	λ6122 absent at K0, K3	Blended with the TiO band in the later types	
		↓ λ6162: its strength relative to TiO is a good indicator of temperature		
	Fe I, Ti I, Cr I λ6362	Absent at K0, K3, very weak or absent at K7	↓	
	CaH λ6386	Present only in the K7 star	Not present	
	Ba II, Fe I, Ca I, Mn I, Ti I, Ti II λ6497	→	→	→
		↓	↓	↓
	Hα λ6563	↑	Present, little variation	
	TiO λ6651-6852	Present only in the K7 and K6 stars		Absent in K0, K3
	TiO λ7053-7270	Present only in the K7 and K6 stars		Present by K3
		Blended with telluric water band		
	K I λ7699	↓	Not present	
	CN λ7878-8068	Present??	→	→
	Ca II λλ8498,8542,8662	→	→	→

TABLE 3
(Continued)

	Feature	Luminosity Class V	Luminosity Class III	Luminosity Class Ib
M0 to M3	Na I λ5893	←	←	←
	TiO, all bands	↓	↓	↓
	Ca I λλ6122,6162	↓ Present in the three spectra. The strength of λ6162 relative to TiO is a good indicator of temperature	Buried in the TiO band	
	Fe I, Ti I, Cr I λ6362	Not present	Present	
	CaH λ6386	Strongest in the M2 (peculiar) star, see text	Not present	
	Ba II, Fe I, Ca I, Mn I, Ti I, Ti II, Ni I λ6497	→	→	→
			↓	↓
	Hα λ6563	Present in all		
	TiO λ6651-6852	←	←	←
	CaH A system λ6750-7050	Strong, blended with TiO and telluric O_2		
	TiO λ7053-7270	Blended with telluric water band		
	Ti I λλ7345,7358,7364	→	→	→
	TiO λ7666-7861	Obvious in our spectra at type M3		
	K I λλ7665,7699	Blended with TiO and telluric O_2	Present??	
	TiO λ8206-8569	Not present	Short wavelengths blended with telluric water band	
	CN λ7878-8068	Not present	→	→
	Na I λλ8183,8195	Blended with telluric water band, but easily distinguished	Confused with telluric water band	
	Ca II λλ8498,8542,8662	→	→	→

†Unfortunately, we lack an observation of the K7 Ib star, so the trends with luminosity for K7 stars, and with temperature for luminosity class Ib are not well established. The spectral changes between K3 Ib and K7 Ib stars, and between K7 III and K7 Ib stars can be drastic. We remind the reader that the K6 III star has been classified by Keenan & McNeil as K7 III (1976, standard star) and K6 III (1989).

While some of these do vary with both parameters, especially in the K and M stars, others were underlined because they are useful to distinguish a whole spectral class. For example, the O I λ7774 line is a good indicator of luminosity, but also helps to distinguish the B1 V from the O9 V in Fig. 4, or the A9 V from the F2 V in Fig. 5. Also notice that some lines may be characteristic of only one of the stars in our spectra. In particular, the C II λ6580 line is present in the B8 Ib star, but not in the adjacent stars B5 Ib, A0 Ib, or B7 III.

Most of the trends described in Table 3 were drawn from the spectra in Figs. 4–22. To corroborate the statements in this table we also used observations that we have taken of other MK spectral types not shown here, as well as papers or atlases published in spectral regions overlapping ours, specially for late-type stars (e.g., Turnshek et al. 1985; Kirkpatrick et al. 1991; MacConnell et al. 1992).

The strength of the Na I λ5893 line is suspect in our spectra, especially when it is weak. It is too close to the edge of the spectra, and calibration points of the standard stars are nonexistent in this region, so the flux values had to be extrapolated. As a result, the continuum slope at wavelengths shorter than this line is not well defined. In addition, this line is contaminated with interstellar Na I, and at the resolution of our observations it is impossible to disentangle the stellar and interstellar contributions.

All main sequence and giant stars later than B1 are practically unaffected by interstellar reddening. Therefore, the continuum slope can also be used as a criterion for distinguishing spectral types, *after* dereddening the spectrum with the appropriate extinction curve. Of course, this may prove to be a difficult task if there is contribution from circumstellar dust.

It is clear from the figures that the Paschen area itself gives a good first approximation of spectral type for early type stars (O–F), especially for A stars. This is completely analogous to the Balmer area in the blue part of the spectrum. For early types, the Paschen area can also distinguish supergiants from luminosity class V or III stars. The Paschen lines in the supergiants are much narrower than in giants or main-sequence stars, so more lines can be resolved in the series. In addition, the O I λ8446 line is a good indicator of luminosity, as is the Paschen jump in A stars. For the late types (G–M), the Paschen area alone (i.e., the Ca II triplet) is a good indicator of luminosity.

The NIR classification system will work if every one of

our program stars can be distinguished from its neighboring stars, both in temperature and luminosity. Below we comment on the MK types that are not so obvious to differentiate at the scale of our figures.

The O4 V can be distinguished from the O6 V because the He lines are weaker in the O4 V star, especially the λ7065 line. Unfortunately the Paschen area is underexposed in the early O stars, so the O6 V, O9 V, O6.5 III, and O9 III stars cannot be differentiated. The NIR classification system is more challenging with O stars than with later ones, plus exposure times can be very long with our instruments even if they are relatively bright in V. The O I λ7774 line is already present at B1, this is the main discriminator between B1 and O9 stars.

The F2 V and F5 V, as well as the F2 III and F5 III stars appear to be very similar, but notice that they are differentiated by the strength of the O I λ7774 line, and more strongly by the relative strength of the Ca II triplet and the Paschen lines.

The G2 V, G5 V, G8 V, and independently the G2 III, G5 III, G8 III stars are the most difficult to distinguish. The λ6497 blend and Hα help to differentiate them. The G8 Ib and K0 Ib stars are separated by the stronger Ca I lines in the G8 Ib star.

Except for the O stars mentioned above, all stars can be distinguished in luminosity, even if only one line is the discriminating factor.

For K and M stars, the classification system in the NIR is extremely useful. It probably will not separate stars to the accuracy of 0.1 subtype (e.g., M3.9), like White and Wing (1978) did in their photometric system, but it may be as good as the MK classification, as Kirkpatrick et al. (1991) have shown for M V and M III stars. We observe in our M-stars spectra that the strength of the TiO band around 5900 Å in the M2 III is stronger than in the M2 V and also than in the M2 Iab–Ib star (Fig. 22). This band is also stronger in the M3 III star than in the M3 V or M3.1 Ib stars, as can be seen by comparing Figs. 7, 11, and 15. Inspection of the spectra of the M2 V, M2 III, and M2 Ib stars in the atlas of Turnshek et al. (1985) reveals the same behavior for this TiO λ5900 band. Although our M2 V program star, G1 15 A, was classified as such by Keenan and McNeil (1989), it is a high-velocity peculiar star. It is also subluminous in absolute magnitude-color diagrams (Spinrad 1973). In the NIR, the best indication that a star is subluminous is enhancement of the CaH band (Boeshaar 1976), an effect which is clearly seen in Fig. 7. Boeshaar (1993) classifies it as dM1.5. Weak TiO may also indicate that a star is subluminous.

As noted before, some lines are sensitive to both temperature and luminosity. An iteration procedure in T and L is needed to assign an MK spectral type, keeping in mind that the whole spectrum must be used in conjunction with that particular line. Also, we still have not investigated other effects which affect the assignment of spectral type and luminosity class, such as metallicity and gravity. For example Xu (1991) found that for G8-M0 stars, the strength of the Ca II triplet increases with increasing metallicity.

The Mg I λ8807 line is another line that can be used as a temperature criterion in F to M stars, but it also depends on metal abundance (Díaz et al. 1989). This is a weak line that falls near the edge of our spectra, where the flux calibration points of the spectrophotometric standards are scarce and poorly determined because of the Paschen lines, so we will not discuss it further.

We have merely presented the red/NIR spectra of stars classified in the MK system, without any attempt to classify them in a NIR system. Of course, it is possible that one or two stars shown here will not fit a red/NIR sequence; this will be the subject of future papers.

5. CONCLUSIONS

We have demonstrated that normal stars follow well-defined patterns in temperature and luminosity in the NIR (5800–8900 Å), at $\sim$15 Å resolution. This wavelength region is most useful for classifying B-type and cooler stars. In fact, for B-type to K-type stars, the Paschen region by itself gives a rough estimate of a star's spectral type. At this point we cannot make any claims about how well a NIR classification system would work for O-type stars.

In particular, supergiants stars are very easily distinguished from giants and main-sequence stars. It has been known for a long time that the O I $\lambda\lambda$7774, 8446 lines are a very helpful luminosity discriminator in A and F stars, and so is the Ca II $\lambda\lambda$8498, 8542, 8662 triplet in A to M stars.

In the papers to follow, we will analyze each spectral class separately (O, B, A, etc.) to see if this NIR system can classify stars to the same accuracy as the MK bins, and will quantify the system by measuring equivalent widths and line ratios.

We thank Dr. Pat Boeshaar for many useful comments pertaining to the M stars, and the referee, Dr. Bob Garrison, for helping us improve this paper. A.V.D. thanks her husband for taking care of their baby while she went observing. This work was supported by the Mericos Foundation and by the National Science Foundation grant No. AST-8914577. We thank the Friends of MIRA for their support.

REFERENCES

Abt, H. A., Meinel, A. B., Morgan, W. W., and Tapscott, J. W. 1968, An Atlas of Low-Dispersion Grating Stellar Spectra
Andrillat, Y. 1979 in IAU Colloq. No. 47, Spectral Classification of the Future, ed. A. G. D. Philip, p. 138
Barbieri, C., Bonoli, C., Bortdetto, F., diSerego, S., and Falomo, R. 1981, Mem. Soc. Astron. Ital. 51, 195
Boeshaar, P. C. 1976, Ph.D. Thesis, The Ohio State University
Boeshaar, P. C. 1993, private communication
Bouw, G. D. 1981, PASP, 93, 45
Breger, M. 1976, ApJS, 32, 7
Danks, A. D., and Dennefeld, M. 1993, preprint
Diaz, A. I., Terlevich, E., and Terlevich, R. 1989, MNRAS, 239, 325
Filippenko, A. V. 1982, PASP, 94, 715

FitzGerald, M. P. 1970, A&A, 4, 234
Garrison, R. F. 1984, The MK Process and Stellar Classification, David Dunlap Observatory (Toronto, Canada)
Gray, R. O., and Garrison, R. F. 1987, ApJS, 65, 581
Gray, R. O., and Garrison, R. F. 1989a, ApJS, 69, 301
Gray, R. O., and Garrison, R. F. 1989b, ApJS, 70, 623
Gunn, J. E., and Stryker, L. L. 1983, ApJS, 52, 121
Hayes, D. S., and Latham, D. W. 1975, ApJ, 197, 599
Hoffleit, D., and Jaschek, C. 1982, The Bright Star Catalog (New Haven, Yale University Observatory)
Johnson, H. L., and Morgan, W. W. 1953, ApJ, 117, 313
Keenan, P. C. 1957, PASP, 69, 5
Keenan, P. C., and Hynek, J. A. 1950, ApJ, 111, 1
Keenan, P. C., and McNeil, R. C. 1976, An Atlas of the Spectra of the Cooler Stars (Columbus, Ohio State University Press)
Keenan, P. C., and McNeil, R. C. 1989, ApJS, 71, 245
Kirkpatrick, J. D., Henry, T. J., and McCarthy, D. W. 1991, ApJS, 77, 417
Lesh, J. R. 1968, ApJS, 17, 371
MacConnell, D. J., Wing, R. F., and Costa, E. 1992, AJ, 104, 821
Massey, P., Boronson, T., Jacoby, G., and Green, R. 1992, NOAO Newsletter No. 32, p. 27
Morgan, W. W., and Keenan, P. C. 1973, ARA&A, 11, 29
Morgan, W., Keenan, P., and Kellman, E. 1943, An Atlas of Stellar Spectra (University of Chicago Press) [MKK]
Morgan, W. W., Abt, H. A., and Tapscott, J. W. 1978, Revised MK Spectral Class for Stars Earlier than the Sun (Yerkes Observatory, University of Chicago and Kitt Peak National Observatory)
Nassau, J. J. 1956, Vistas in Astronomy, ed. A. Beer (New York, Pergamon), Vol. 1, p. 1361
Parsons, S. B. 1964, ApJ, 140, 853
Schulte-Ladbeck, R. E. 1988, A&A, 189, 97
Sharpless, S. 1956, ApJ, 124, 342
Spinrad, H. 1973, ApJ, 183, 923
Tüg, H., White, N. M., and Lockwood, G. W. 1977, A&A, 61, 679
Turnshek, D. E., Turnshek, D. A., Craine, E., and Boeshaar, P. C. 1985, An Atlas of Digital Spectra of Cool Stars (Tucson, Western Research Company)
Walborn, N. R. 1971, ApJS, 23, 257
Walborn, N. R. 1973, AJ, 78, 1067
White, N. M., and Wing, R. F. 1978, ApJ, 222, 209
Wing, R. F. 1970, in Proc. of the Conference on Late Type Stars, ed. G. E. Lockwood and H. M. Dyck, KPNO Contribution No. 554, p. 145
Xu, Z. 1991, A&A, 248, 367